42p.

# INFRASONIC WAVES
# FROM
# THE AURORAL ZONE

(NASA TMX 54620;

DECEMBER 1963

auths:
Kaichi Maeda and Tomiya Watanabe (Brit.
Columbia U.) Dec. 1963. 42p refs Presented
at the Am. Geophys. Union Ann. meeting in Apr.
1962    Submitted for publication
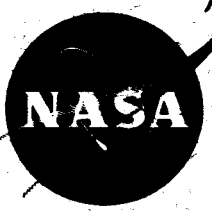
**NASA** GODDARD SPACE FLIGHT CENTER,
GREENBELT, MARYLAND

# INFRASONIC WAVES FROM THE AURORAL ZONE

by
Kaichi Maeda
*Goddard Space Flight Center*

and

Tomiya Watanabe
*University of British Columbia*

$17690$ **SUMMARY** *ABST*

Pulsating aurorae are proposed as a source of the infrasonic waves associated with geomagnetic activity reported by Chrzanowski et al. One of the most plausible generation mechanisms of these long period pressure waves is the periodic heating of the air around 100 km, corresponding to the auroral coruscation reported by Campbell and Rees. In order to show the energetic relationship between source input and pressure change at sea level, some theoretical calculations are performed by using a simple model of auroral distribution in the isothermal atmosphere.

*AUTHOR*

# CONTENTS

# INFRASONIC WAVES FROM THE AURORAL ZONE

by
Kaichi R. Maeda
*Goddard Space Flight Center*

and

Tomiya Watanabe
*University of British Columbia*

## INTRODUCTION

The purpose of this paper is to interpret the origin of the strange traveling atmospheric waves observed at the ground during intervals of high geomagnetic activity (Reference 1). In particular, discussion centers on possible modes of atmospheric oscillations caused by the periodic bombardment of auroral particles in the polar mesosphere.

Trains of the waves are detected by a system of four microphones placed on each corner of a quadrant roughly 8 km square, located north of Washington, D. C. The presence of a traveling wave is established when the same wave forms can be found on all four records with certain time shifts between them. These time displacements are used to determine the direction of wave propagation and the horizontal phase velocity of the waves. The periods of these infrasonic waves are usually 20 to 80 sec, but occasionally 100 to 300 sec waves are recorded. The pressure amplitude ranges from about 1 to 10 dynes/cm$^2$.

One of the peculiar features of these waves is the change of arrival direction with time of day. The general trend is from the northeast in the evening, from the north about midnight, and from the northwest in the morning. The shift back to northeast is somewhat discontinuous. These waves occur less frequently in the daytime.

Since auroral activity predominates at about midnight local time, the time dependence of the appearance of infrasonic waves during intervals of high geomagnetic activity can be explained by assuming that the source of this kind of wave is located somewhere in the auroral region, as can be seen from Figure 1. The left side of this figure shows the diurnal variation of the arrival of sound waves during magnetic storms, reported by Chrzanowski et al. (Reference 1). This assumption is consistent with the finding that the enhancement of the wave intensity at Washington, D. C. is generally delayed several hours after the increase of geomagnetic activity, except in the case of very severe magnetic storms. During these storms the delay is less than 30 minutes, indicating sourthward spread of the source of these waves near Washington, D. C.
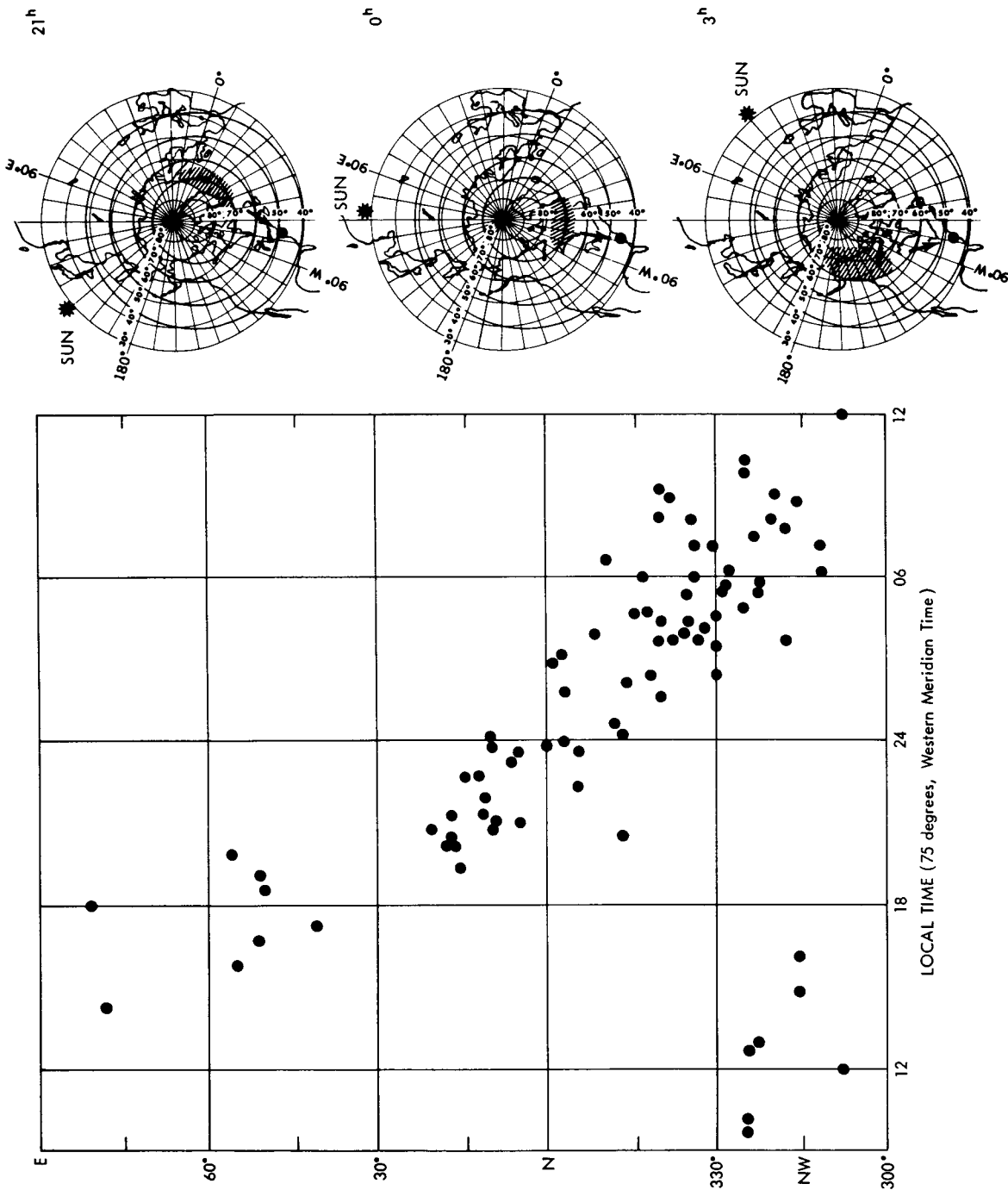
Figure 1—Diurnal variation of the arrival direction of infrasonic waves during magnetic storms observed at the National Bureau of Standards, Washington, D. C. The three figures on the right indicate the shifts of the source of the pressure waves, corresponding to the movement of auroral activity.

In attempting to understand these peculiar pressure waves, it is proposed that they originate from a certain domain of the ionospheric region in the auroral zone which is heated periodically by a severe bombardment of auroral particles. It is thought that this periodic precipitation of auroral particles occurs simultaneously with geomagnetic pulsations.

## INTERRELATIONS BETWEEN GEOMAGNETIC FLUCTUATIONS, PULSATING AURORAE, AND INFRASONIC WAVES

The auroral luminosity often fluctuates with incoming auroral particles. The fluctuations of these particles, mostly electrons, can be explained by either a periodic change in the acceleration mechanism of incident particles or by the change of mirror heights of trapped particles in the earth's atmosphere, following the variations of the field intensity of the earth's magnetosphere. The variations of geomagnetic field intensity and of auroral brightness are therefore closely related. A clear example of the correspondence between the pulsating aurorae and the rapid variation of geomagnetic intensity observed at the ground has been given by Campbell (Reference 2).

According to the analysis of the space probe data given by Sonnet et al. (Reference 3), and that of Explorer X (1961 κ1) given by Heppner et al. (References 4 and 5), the region near the geomagnetic equator beyond about 10 earth radii is occasionally greatly disturbed. Such disturbances may be propagated along the magnetic lines of force as hydromagnetic waves, and are transformed into electromagnetic waves when they reach the conducting ionosphere (References 6-8). After penetrating the ionospheric region as electromagnetic waves, they are almost perfectly reflected at the earth's surface (Reference 9). This produces standing hydromagnetic waves along magnetic lines of force. The simplest mode of such standing waves is the fundamental mode, whose unique node is on the geomagnetic equatorial plane, with two loops of oscillation on the ends of the line of force on the earth, one in each hemisphere. This mode of oscillation has been investigated theoretically by Dungey (Reference 10), who called it the normal mode of torsional oscillations of the magnetic field in the earth's cavity. The eigen period of these oscillations increases rapidly with the latitude of the magnetic line of force intersecting the earth's surface, varying from several tens of seconds in the subauroral region to about 10 minutes in the polar region (References 11-13).

In addition to the above mode, there is another mode of oscillation responsible for geomagnetic pulsations of shorter periods. As noted by Dessler (Reference 14), the velocity of Alfvén waves decreases very rapidly with decreasing height in the exospheric region below around 2,000 km. Therefore, because of the continuity of energy flow Alfvén waves of certain periods coming from the outer exosphere can be expected to be intensified. In this mode of oscillation, the layer of maximum Alfvén velocity, approximately between 1500 and 3000 km, becomes the node of oscillation, and the loop of oscillation is near the earth's surface. This mode of hydromagnetic oscillation corresponds to the geomagnetic pulsations with periods from about 1 to several seconds, which appear more frequently in nighttime than in daytime (Reference 15).

In considering the above facts, it might be speculated that a possible mechanism for the production of infrasonic waves during auroral activity would be the penetration of Alfvén waves,

including modified Alfvén waves and retarded sound waves (Reference 13), through the ionosphere. However, as will be shown later, these contributions are very small compared with the pressure disturbances produced by the periodic heating of the lower ionosphere caused by auroral bombardments.

As shown by Heppner (Reference 16) auroral activity predominates around midnight local time and the active region extends towards lower latitudes with increasing activity; pulsating aurorae appear at this phase of auroral activity. In other words, among several types of auroral displays pulsating aurorae appear with the largest disturbance in energy and they occur in fairly low latitudes.

According to Campbell and Ress (Reference 17) the peak of pulsating aurorae is around 100 km, the bottom is at 90 km, the effective thickness is of the order of 20 km, and the most frequent period is from 6 to 10 sec. From the direct measurement of auroral particles by means of rocket borne detectors, the energy flux of auroral particles, mostly electrons, is of the order of several tens of ergs/cm$^2$-sec at weak aurora and increases by more than a factor of 50 at bright aurora (Reference 18). Thus, the energy flux in a strong pulsating aurora can be estimated to be of the order of $10^3$ ergs/cm$^2$-sec or more. This figure is consistent with the estimate given by Chamberlain (Reference 19), based on measurements of auroral luminosity.

On the other hand, the energy flux of hydromagnetic waves deduced from the magnetic pulsation data is less than 10 ergs/cm$^2$-sec below 200 km. The energy flux of hydromagnetic waves increases with height. However, the contribution to pressure waves in the lower atmosphere decreases with the increasing height of the source, as will be shown later.

Another evidence for the present idea is the very good correspondence between the appearance of pulsating aurorae and that of infrasonic waves (Figure 2). The occurrence of pulsating aurorae shown on the right of Figure 2 is taken from the visoplot of auroral activity, reported by IGY World Data Center A, on days which correspond to the events, reported by Chrzanowski et al. (Reference 1), shown on the left of this figure. Two occurrences of infrasonic waves in 1957 were reported, but since no visoplots of auroral activity are available before the IGY, they are omitted from this figure. The arrival direction of these waves might deviate from their true direction because of strong wind systems in high altitudes. Therefore, the appearances of pressure waves do not necessarily match the pulsating auroral events in detail. However, it is quite clear that there is a close correspondence between infrasonic waves and pulsating aurorae.

## MATHEMATICAL TREATMENT

It is obvious that ray theory is not applicable in this problem, because the wavelength is of the order of an atmospheric depth or more for the infrasonic waves observed.

The excitation and propagation of long period pressure waves in the atmosphere have been investigated by several workers, mainly in two fields of geophysics, i.e., meteorology and ionospheric physics. The former consists of the study of atmospheric oscillations (References 20-24),

4

Figure 2—Diurnal variation of the arrival direction of infrasonic waves during specific magnetic storms detected at the National Bureau of Standards, Washington, D. C. (Chrzanowski et al., 1960), and corresponding auroral activities observed in the northern hemisphere.

and the study of micro-barometric disturbances (References 25-36). The latter is mostly concerned with the investigation of ionospheric disturbances and has been discussed by Martyn (Reference 37), Sen and White (Reference 38), White (References 39 and 40) and Hines (References 41 and 42).

Although the subjects considered in the noted references are quite different, the mathematical treatments are essentially the same. They are based on a differential equation of velocity divergence, which is derived from three fundamental equations, i.e., the equations of motion, continuity, and of first law of thermodynamics. The theoretical aspects of the problems in geophysics, including oceanography, are reviewed in References 43-46. Mathematical technique has been developed to solve these problems, introducing the so-called field variables instead of simple hydrodynamical variables.

In the present calculations, however, the classical method based on the equations of velocity divergence will be used, because of the convenience in comparing the results with observed data.

5

## Notations and Fundamental Equations

Preliminary notation will now be given:

$c$    velocity of sound in the atmosphere in cm/sec, $c^2 = \gamma g H$ where $H = RT/g$ is the scale height of the isothermal atmosphere,

$D/Dt$    Eulerian derivative, $\partial/\partial t + U\nabla$,

$f$    resultant of external forces except gravity, dynes/gm,

$g(0, -g)$    acceleration of gravity, $g = 980$ cm/sec$^2$,

$k$    horizontal wave number corresponding to $\lambda$, in cm$^{-1}$, i.e., $2\pi/\lambda$,

$l$    vertical wavelength of a pressure wave in cm,

$p, \rho, T$    small departures from static values of pressure, density, and temperature, functions of $x$, $z$, and $t$, in dynes/cm$^2$, gm/cm$^3$, and °K,

$p_0, \rho_0, T_0$    static values of pressure, density, and temperature, functions of $z$ only,

$p_s, \rho_s, T_s$    static values of pressure, density, and temperature of air at sea level,

$p_T, \rho_T, T_T$    total pressure, density, and temperature, i.e., $p_0 + p$, $\rho_0 + \rho$, and $T_0 + T$,

$q'(x, z)$    rate of net accession of heat, erg/gm-sec; $s(x, z) = (\gamma - 1)q$ where $q = \rho_T q'$ in ergs/cm$^3$-sec,

$R$    gas constant of air, $B/M = 2.87 \times 10^6$ ergs/gm-°C, where $B$ is the universal gas constant, $8.314 \times 10^7$ ergs/mol-°K, and $M$ is the molecular weight of air, approximately 28.97,

$U(u, w)$    velocity vector, where $u$ is the horizontal (southward) and $w$ is the upward component of air flow in cm/sec,

$x, z$    horizontal (southward) and vectical (upward) coordinates,

$\gamma$    ratio of the specific heats of air, $C_p/C_v \approx 1.4$, where $C_p$ and $C_v$ are the specific heat of air at constant pressure and constant volume, respectively,

$\eta$    entropy of air in ergs/gm-°K,

$\lambda$    horizontal wavelength of a pressure wave in cm,

$\sigma$    frequency of the pressure wave corresponding to $\tau$, i.e., $2\pi/\tau$,

$\tau$    period of pressure wave in sec,

$\chi(x, z)$    the divergence of velocity in sec$^{-1}$, i.e., $\chi = \partial u/\partial x + \partial w/\partial z$,

$\Omega$    Coriolis vector in rad/sec.

In Eulerian notation, the equation of motion is

$$\frac{DU}{Dt} + \frac{1}{\rho}\nabla p + g + \Omega \times U = f \quad , \tag{1}$$

and the equation of continuity is

$$\frac{D}{DT}\left(\frac{1}{\rho}\right) - \frac{1}{\rho}\nabla U = 0 \tag{2}$$

The variations of pressure due to thermal excitations can be derived from the first law of thermodynamics, which gives the change of entropy (References 43-45),

$$\frac{D\eta}{Dt} = \frac{q'}{T} . \tag{3}$$

By making use of the perfect gas function for entropy (Reference 46) it can be shown that Equation 3 is equivalent to

$$\frac{Dp}{Dt} - c^2 \frac{D\rho}{Dt} = s(x, z, t) , \tag{4}$$

where

$$s(x, z, t) = (\gamma - 1)\rho q'(x, z, t) = (\gamma - 1)q(x, z, t) . \tag{5}$$

Since, in the present problem, the period of oscillation is less than a few minutes, the Coriolis force due to the earth's rotation is negligible, and all other external forces can be assumed to be zero. The equation of motion for the present problem is then simply

$$\frac{DU}{Dt} + \frac{1}{\rho_0}\nabla p = g . \tag{6}$$

## One-Dimensional Model

For the one-dimensional case atmospheric motion has only the $z$ component of velocity, $w$; therefore, in its linear approximation form, the equation of motion (Equation 6) is

$$\rho_0 \frac{\partial w}{\partial z} = \frac{-\partial p}{\partial z} - \rho g . \tag{7}$$

The equation of continuity in its linear approximation form is

$$\frac{\partial \rho}{\partial t} + \rho_0 \frac{\partial w}{\partial z} - \frac{\rho_0}{H} w = 0 . \tag{8}$$

And the linear approximation form of the entropy equation (Equation 4) is:

$$\frac{\partial p}{\partial t} = -\rho_0 c^2 \frac{\partial w}{\partial z} + \rho_0 gw + (\gamma - 1)q , \tag{9}$$

where $q = q(z, t)$ is the periodically changing heat source, which can be assumed to be

$$q(z, t) = \begin{cases} q(z) e^{i\sigma t} & \text{for } z \geq 0 \ , \\ \\ 0 & \text{for } - z_0 \leq z < 0 \ , \end{cases} \tag{10}$$

where

$$q(z) = \frac{q_0 e^{-z/h}}{h} \ ; \tag{11}$$

$h$ is a constant and $q_0$ is the maximum rate of heat generation in an atmospheric column with unit cross section, in ergs/cm$^2$-sec; $z = 0$ is taken as the height of the base of heating; and the value at the earth's surface is given by $z = - z_0$ .

By eliminating $p$ and $\rho$ from the above equations, the following differential equation is obtained:

$$\frac{\partial^2 w}{\partial z^2} - \frac{1}{H} \frac{\partial w}{\partial z} - \frac{1}{c^2} \frac{\partial^2 w}{\partial t^2} = \frac{\gamma - 1}{\rho_0 c^2} \frac{\partial q}{\partial z} \ . \tag{12}$$

In the region $z \geq 0$, where the heat source exists,

$$w = \frac{i}{k_2 - k_1} e^{ik_1 z} \left[ \int_0^z e^{-ik_1 \xi} Q(\xi) \, d\xi + C \right] + \frac{i}{k_1 - k_2} e^{ik_2 z} \left[ \int_0^z e^{-ik_2 \xi} Q(\xi) \, d\xi + D \right] \ , \tag{13}$$

where $k_1$ and $k_2$ are given by

$$\left. \begin{aligned} k_1 &= \sqrt{\frac{1}{l^2} - \frac{1}{4H^2}} - i \frac{1}{2H} \ , \\ \\ k_2 &= - \sqrt{\frac{1}{l^2} - \frac{1}{4H^2}} - i \frac{1}{2H} \ , \end{aligned} \right\} \tag{14}$$

and

$$\frac{1}{l} = \frac{\sigma}{c} \ ,$$

$$Q(\xi) = \frac{\gamma - 1}{\rho_0 c^2} \frac{dq(\xi)}{d\xi} \ . \tag{15}$$

C and D are integration constants, to be determined by the boundary conditions. The time-dependent factor, $e^{i\sigma t}$, is dropped in Equation 13 and will be always dropped hereafter.

8

For the region $-z_0 \leq z < 0$, where no heat source exists,

$$w = \frac{i}{k_2 - k_1} e^{ik_1 z} A + \frac{i}{k_1 - k_2} e^{ik_2 z} B \quad ; \tag{16}$$

where A and B are constants. The condition that $w = 0$ at the earth's surface gives

$$B = e^{i(k_2 - k_1)z_0} A \quad . \tag{17}$$

The vertical velocity $w$ should be continuous at $z = 0$, and therefore

$$A - B = C - D \quad . \tag{18}$$

The pressure $p$ also should be continuous at $z = 0$, so that the following condition is to be satisfied:

$$\rho_c c^2 \left(\frac{dw}{dz}\right)_{z=0+\epsilon} - (\gamma - 1) q(0) = \rho_c c^2 \left(\frac{dw}{dz}\right)_{z=0-\epsilon} \quad , \tag{19}$$

where $\bullet \to 0$ and

$$\rho_c = \left(\rho_0\right)_{z=0} \quad , \tag{20}$$

the atmospheric density at $z = 0$.

The above equations give

$$k_1 C - k_2 D - k_1 A + k_2 B = \frac{k_1 - k_2}{\rho_c c^2} (\gamma - 1) q(0) \quad . \tag{21}$$

For $z \to \infty$, there should be no wave downward, thus from Equation 13

$$C = -\int_0^\infty e^{-ik_1 \xi} Q(\xi) d\xi \quad . \tag{22}$$

From Equations 18 and 19,

$$A = C - \frac{\gamma - 1}{\rho_c c^2} q(0) \quad . \tag{23}$$

9

To find the pressure variation at the earth's surface, we must obtain $\left(dw/dz\right)_{z=-z_0}$, which is given by using Equations 16 and 17;

$$\left(\frac{dw}{dz}\right)_{z=-z_0} = e^{-ik_1 z_0} A \quad .$$ (24)

Then Equation 9 gives the pressure variation at the earth's surface,

$$P_{z=-z_0} = \frac{i}{\sigma} \rho_s c^2 e^{-ik_1 z_0} A \quad ,$$ (25)

where $\rho_s$ is the atmospheric density at the earth's surface. By substituting Equation 22 into Equation 23,

$$|A| = \frac{(\gamma-1) q_0}{\rho_c c^2} \frac{1}{l} \left(1 - \frac{h}{H} + \frac{h^2}{l^2}\right)^{-1/2} \quad ,$$ (26)

provided that the angular wave frequency $\sigma$ is larger than a critical frequency $\sigma_A$,

$$\sigma_A = \frac{\gamma g}{2c} \quad .$$ (27)

By using Equations 14

$$\left|e^{-ik_1 z_0}\right| = e^{-z_0/2H} \quad .$$ (28)

Thus the final expression of the amplitude of pressure variations at the ground, caused by the periodic disturbance in the upper atmosphere $q(z, t)$, is

$$P_s = \frac{\gamma-1}{c} q_0 \left(\frac{\rho_s}{\rho_c}\right)^{1/2} \left(1 - \frac{h}{H} + \frac{h^2}{l^2}\right)^{1/2} \quad .$$ (29)

The values for $P_s/q_0$ which may be derived from this equation are plotted vs. $h$ in Figure 3 for several values of angular frequency, $\sigma$. The full lines and dashed lines stand for the scale heights of 8 km and 6.8 km, respectively, for an isothermal atmosphere. The latter gives the proper ratio of $\left(\rho_c/\rho_s\right)^{1/2}$ as compared with the observed atmospheric densities. From this figure, it can be seen that periodic heating corresponding to a flux of the order of 100 ergs/cm²-sec produces pressure waves with amplitudes of the order of 1 dyne/cm² at the ground.

10

## Two-Dimensional Model

*Equation of Velocity Divergence*

From Equation 6 the equation of motion for the two-dimensional case is

$$\rho_0 \frac{\partial u}{\partial t} = -\frac{\partial p}{\partial x} \quad , \tag{30}$$

$$\rho_0 \frac{\partial w}{\partial t} = -\frac{\partial p}{\partial z} - g\rho \quad . \tag{31}$$

The equation of continuity (Equation 2) can be written in a first order approximation as

$$\frac{\partial p}{\partial t} + w \frac{\partial \rho_0}{\partial z} = -\rho_0 \chi \quad , \tag{32}$$
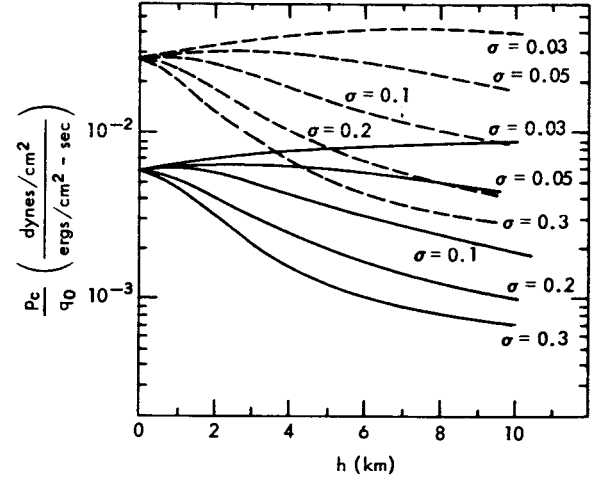


Figure 3—Relative intensity of pressure waves on the ground, produced by periodic auroral heating, vs. the scale height of the heat source, for the one-dimensional model with an isothermal atmosphere.

where $\chi = \chi(x, z, t)$ is the velocity divergence. By using Equation 32, Equation 4 can be written as

$$\frac{\partial p}{\partial t} = \rho_0 g w - \rho_0 c^2 \chi + s \quad . \tag{33}$$

Under the assumption that the time variations of $u, w, p, \rho$, and $s$ are proportional to a factor $e^{i\sigma t}$, the following relations between $u, w$, and $p$ are obtained from Equations 30-33:

$$-\sigma^2 u = \frac{\partial}{\partial x}\left(c^2 \chi - gw\right) - \frac{1}{\rho_0} \frac{\partial s}{\partial x} \quad , \tag{34}$$

$$-\sigma^2 w = c^2 \frac{\partial \chi}{\partial z} - \gamma g \chi + g \frac{\partial u}{\partial x} - \frac{1}{\rho_0} \frac{\partial s}{\partial x} \quad , \tag{35}$$

$$i\sigma p = \rho_0 g w - c^2 \rho_0 \chi + s \quad . \tag{36}$$

By eliminating $u, w$, and $p$ from these equations, the following differential equation for the velocity divergence $\chi(x, z)$ is obtained:

$$\nabla^2 \chi + \frac{1}{c^2}\left(\frac{dc^2}{dz} - \gamma g\right)\frac{\partial \chi}{\partial z} - \frac{g}{c^2 \sigma^2}\left[\frac{dc^2}{dz} + (\gamma - 1) g\right]\frac{\partial^2 \chi}{\partial x^2} + \frac{\sigma^2}{c^2}\chi$$

$$= -\frac{1}{c^2 \sigma^2}\left[\frac{g}{\rho_0(z) c^2}\left(\frac{dc^2}{dz} + \gamma g\right)\frac{\partial^2 s}{\partial x^2} - \frac{\sigma^2}{\rho_0 c^2}\left(\frac{dc^2}{dz} + \gamma g\right)\frac{\partial s}{\partial z} - \frac{\sigma^2}{\rho_0}\nabla^2 s\right] \quad . \tag{37}$$

The derivation of this equation is given in Appendix A.

*The Diagnostic Diagram*

If there is no thermal excitation, the right side of Equation 37 is zero, and the solution of this homogenous differential equation corresponds to the free oscillation of the atmosphere on the nonrotating earth.

We will now consider pressure waves traveling horizontally in this flat atmosphere. If $u$, $w$, $p$, and $\rho$ are proportional to a factor $e^{i(\sigma t - kx)}$, the following is the equation for the vertical change of $\chi(\sigma, z)$:

$$\frac{d^2 \chi}{dz^2} + \frac{1}{c^2}\left(\frac{dc^2}{dz} - \gamma g\right)\frac{d\chi}{dz} + \left[\frac{\sigma^2}{c^2} - k^2 + \frac{gk^2}{\sigma^2 c^2}\left(\frac{dc^2}{dz} + \gamma g - g\right)\right]\chi = 0 \quad . \tag{38}$$

Since $c^2 = \gamma g H(z)$, this may be written

$$\frac{d^2 \chi}{dz^2} + \frac{1}{H}(H' - 1)\frac{d\chi}{dz} + \left[\frac{\sigma^2}{\gamma g H} - k^2 + \frac{k^2 g}{\sigma^2 H}\left(H' + \frac{\gamma - 1}{\gamma}\right)\right]\chi = 0 \quad , \tag{39}$$

where $H' = dH/dz$ .

For simplicity, consider the case of an isothermal atmosphere, where $H' = 0$. Equation 39 becomes

$$\frac{d^2 \chi}{dz^2} - 2N\frac{d\chi}{dz} + M^2 \chi = 0 \quad , \tag{40}$$

where the constant $N = 1/2H$ and

$$M^2 = \frac{\sigma^2}{c^2} - k^2 + \frac{k^2 g^2}{c^2 \sigma^2}(\gamma - 1) \quad . \tag{41}$$

This differential equation has the solution:

$$\chi(\sigma, z) = e^{Nz}\left(Ae^{-\mu z} + Be^{+\mu z}\right) \quad , \tag{42}$$

where $A$ and $B$ are constants,

$$\mu^2 = N^2 - M^2 \geq 0 \quad , \tag{43}$$

for the noncellular solution, and

$$\mu = i\eta \quad , \qquad \eta^2 = M^2 - N^2 > 0 \quad , \tag{44}$$

12

for the cellular solution. As was shown by Pekeris (Reference 27) for the noncellular solution in an isothermal atmosphere (Equation 42) the term with $e^{\mu z}$ must vanish, i.e., $B = 0$. Otherwise the kinetic energy of noncellular waves, which is proportional to $\rho_0 (z) \chi^2$, would diverge. Furthermore, because of the condition that the vertical component of velocity must vanish at the ground, we get only two possible types of free oscillation, specified by the following characteristic relations:

Type I: 
$$k = \frac{\sigma}{c} , \qquad V = U = c , \quad \text{and} \quad \mu = \frac{g(2 - \gamma)}{2c^2} , \qquad (45)$$

Type II: 
$$k = \frac{\sigma^2}{g} , \qquad V = \frac{g}{\sigma} U = \frac{1}{2} V , \quad \text{and} \quad \mu = \frac{\sigma^2}{g} - \frac{\gamma g}{2c^2} , \qquad (46)$$

where $V = \sigma/k$ and $U = d\sigma/dk$, the phase velocity and group velocity of noncellular horizontal waves. Type I corresponds to Lamb's wave (Reference 20), which exists at all frequencies; the waves of type II can be propagated only above a critical value $\sigma_c$,

$$\sigma_c = \frac{g}{c} \sqrt{\frac{\gamma}{2}} \qquad (47)$$

(the corresponding period is about 250 sec), and the wave is dispersive.

It should be noted that, because of the decrease of atmospheric density, the amplitude of the Lamb wave (pressure variation) decreases with altitude by a factor $\exp\left(- gz/c^2\right)$, preventing the propagation of waves in any except horizontal directions (Reference 46). On the other hand, for the cellular solution $\eta$ stands for the wave number in the vertical direction and Equation 44 is equivalent to

$$\eta^2 c^2 = \frac{\left(\sigma^2 - \sigma_A^2\right) + k^2 c^2 \left(\sigma_B^2 - \sigma^2\right)}{\sigma^2} , \qquad (48)$$

where

$$\sigma_A = \frac{g\gamma}{2c} ,$$

$$\sigma_B = \frac{g(\gamma - 1)^{1/2}}{c} . \qquad (49)$$

Brunt's frequency, $\sigma_B$, is the frequency of the vertical oscillation of a free air parcel in the atmosphere, changing adiabatically. This expression was also derived by Väisälä as a stability parameter of the atmosphere (Reference 46). The frequency $\sigma_A$ can be called the atmospheric resonance sound frequency (Reference 47).

The curve for $\eta^2 = 0$ shown in Figure 4 (a plot of $\sigma$ vs. $k$) consists of two branches, A and B. The curve A starts from the $\sigma$-axis at $\sigma = \sigma_A$ and is asymptotic to the line C, which corresponds
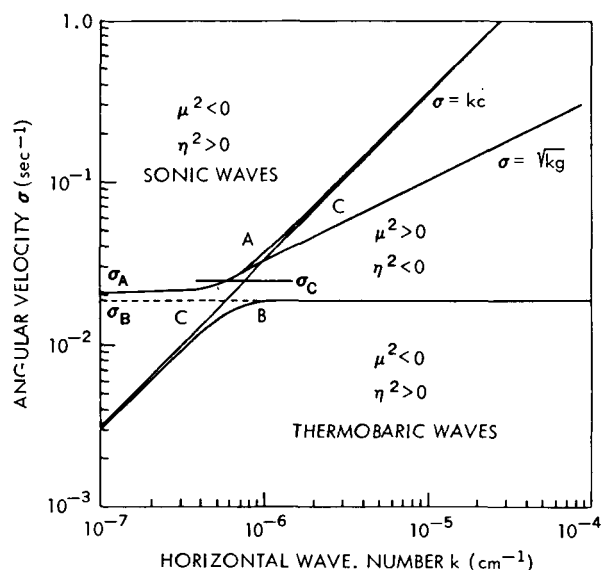
Figure 4—Diagnostic diagram for an isothermal atmosphere with scale height H = 8 km ($T_0$ = 273 °K).

to the solution of the noncellular Lamb wave, $\sigma = kc$. The other curve B passes through the origin and is asymptotic to the horizontal line $\sigma = \sigma_B$. Every point in the two regions where $\eta^2 > 0$, one surrounded by curve A and the other surrounded by curve B, leads to an eigen solution of Equation 39. In the third region (between the other two), where $\eta^2 < 0$, only the points on the line $\sigma = kc$ and $\sigma = \sqrt{kg}$ $(\sigma > \sigma_c)$ lead to eigen solutions. Figure 4 is called the diagnostic diagram of the isothermal atmosphere, and the waves corresponding to the two domains in which $\eta^2 > 0$ are named Sonic (mode A) and Thermobaric (mode B), respectively (Reference 46). Sonic and thermobaric waves are called acoustic and internal gravity waves, respectively, by Hines (Reference 42).

*Intensity of Pressure Waves at the Ground*

Since the source of excitation $s(x, z)$ is limited to a certain area inside the auroral zone, the right side of Equation 37 is not uniform with respect to $x$. Therefore, this differential equation is not in general separable with respect to the variables $x$ and $z$, and the following assumptions are made in solving the equation:

1. The atmosphere is isothermal, with scale height H, in km.

2. The distribution of the heat source is uniform along the $y$ direction (this is assumed at the beginning to reduce the problem to two dimensions), but it is limited horizontally in the $x$ direction within $\pm\lambda_0$ (i.e., $-\lambda_0 \leq x < \lambda_0$ ) and is extended vertically above a certain height $z$ (i.e., $z \geq z_0$).

3. The time variation of the heat source is periodic with an angular frequency $\sigma$, and the same phase within the domain indicated in item 2 above.

The first assumption reduces Equation 37 to the following form:

$$\left(1 - \frac{\sigma_B^2}{\sigma^2}\right)\frac{\partial^2 \chi}{\partial x^2} + \frac{\partial^2 \chi}{\partial z^2} - \frac{1}{H}\frac{\partial \chi}{\partial z} + \frac{\sigma^2}{c^2} \chi$$

$$= \frac{1}{\rho_0(z)c^2} \left[\left(1 - \frac{g}{\sigma^2 H}\right)\frac{\partial^2 s}{\partial x^2} + \frac{\partial^2 s}{\partial z^2} + \frac{1}{H}\frac{\partial s}{\partial z}\right] . \tag{50}$$

Assumptions 2 and 3 can be written as

$$s(x, z, t) = s(z) e^{i\sigma t} \theta(z - z_0) \left[\theta(x + \lambda_0) - \theta(x - \lambda_0)\right] , \tag{51}$$

14

where

$$s(z) = \frac{s_0}{h} e^{-(z-z_0)/h} = \frac{(\gamma - 1) q_0}{h} \exp\left[\frac{-(z - z_0)}{h}\right] \quad , \tag{52}$$

and $\theta(\xi)$ is a unit step function of $\xi$,

$$\theta(\xi) = \begin{cases} 1 & \text{for } \xi \geq 0 \quad , \\ 0 & \text{for } \xi < 0 \quad . \end{cases} \tag{53}$$

It should be noted that $q_0$ is the maximum rate of heat release in the atmosphere in an air column of unit cross-section (in ergs/cm$^2$-sec).

Since the atmosphere is assumed to be isothermal, the density of air in equilibrium at height $z$ is

$$\rho_0(z) = \rho_s e^{-z/H} \quad , \tag{54}$$

where $\rho_s$ is the atmospheric density at the earth's surface and $H$ is the scale height.

In order to solve Equation 50 under the conditions listed, the following Fourier transforms are applied with respect to $x$,

$$X(k, z) = \frac{1}{\sqrt{2\pi}} \int_{-\infty}^{\infty} e^{ikx} \chi(x, z) \, dx \quad , \tag{55}$$

$$S(k, z) = \frac{1}{\sqrt{2\pi}} \int_{-\infty}^{\infty} e^{ikx} s(x, z) \, dx \quad . \tag{56}$$

Since the heat source $s(x, z)$ vanishes outside of the auroral zone, both $s(x, z)$ and $\chi(x, z)$ must vanish at $x = \pm\infty$. Thus

$$\frac{1}{\sqrt{2\pi}} \int_{-\infty}^{\infty} \frac{\partial^2 \chi}{\partial x^2} e^{ikx} \, dx = -k^2 X(k, z) \quad , \tag{57}$$

$$\frac{1}{\sqrt{2\pi}} \int_{-\infty}^{\infty} \frac{\partial^2 s}{\partial x^2} e^{ikx} \, dx = -k^2 S(k, z) \quad . \tag{58}$$

With these transforms, Equation 50 is written

$$\frac{d^2 X}{dz^2} - 2N\frac{dX}{dz} + M^2 X = F(z, k) \quad , \tag{59}$$

where

$$F(z, k) = \frac{1}{c^2 \rho_0(z)}\left[\frac{d^2 S}{dz^2} + \frac{1}{H}\frac{dS}{dz} - k^2\left(1 - \frac{g}{\sigma H}\right)S\right] \quad , \tag{60}$$

and $N$ and $M^2$ are the same as in Equations 40 and 41. The solution of Equation 59 can be written:

$$X(k, z) = e^{n_1 z}\left[C_1 - \frac{1}{2\mu}\int_0^z F(z', k) e^{-n_1 z'} dz'\right] + e^{n_2 z}\left[C_2 + \frac{1}{2\mu}\int_0^z F(z', k) e^{-n_2 z'} dz'\right] \quad , \tag{61}$$

where $F(z', k)$ is given by Equation 60 and $n_1$ and $n_2$ are the roots of the characteristic equation

$$n^2 - 2Nn + M^2 = 0 \quad . \tag{62}$$

We assume

$$n_1 = N - \mu \quad , \tag{63}$$

$$n_2 = N + \mu \quad , \tag{64}$$

where

$$\left.\begin{array}{ll} \mu = \sqrt{N^2 - M^2} \geq 0 & \text{for } N^2 \geq M^2 \quad , \\[2ex] \mu = i\eta, \quad \eta^2 = M^2 - N^2 > 0 & \text{for } N^2 < M^2 \end{array}\right\} \quad . \tag{65}$$

The integration constants $C_1$ and $C_2$ are determined by the following two boundary conditions:

1. The vertical component of velocity vanishes at the ground,

$$w(x, z = 0) = 0 \quad . \tag{66}$$

2. The kinetic energy of the waves at $z = \infty$ is either zero or remains finite. In the latter case, the vertical component of the disturbance should never be propagated downward at $z = \infty$.

The pressure change at the ground can be obtained from $\chi(x, z = 0)$, which is given by the inverse Fourier transform of $X(k, z = 0)$, i.e.,

$$\chi(x, 0) = \frac{1}{\sqrt{2\pi}} \int_{-\infty}^{\infty} e^{-ixk} X(k, 0) dk \quad , \tag{67}$$

where $X(k, 0)$ is the solution of Equation 59 at $z = 0$ satisfying the above conditions. It is given by Equation B15 in Appendix B.

Since $w(x, 0) = 0$, then $s(x, 0) = 0$ and Equation 36 reduces to

$$p(x, 0) = -\frac{c^2 \rho_s}{i\sigma} \chi(x, 0) \quad , \tag{68}$$

where $\chi(x, 0)$ is given by the inverse Fourier transform of $X(k, 0)$. The evaluations of $p(x, 0)$ are given in Appendix C and the results are shown in Figures 5-10. Various values are given in Tables 1 and 2. The symbols $p_r$ and $p_i$ signify the real and imaginary parts of the cellular mode, respectively.
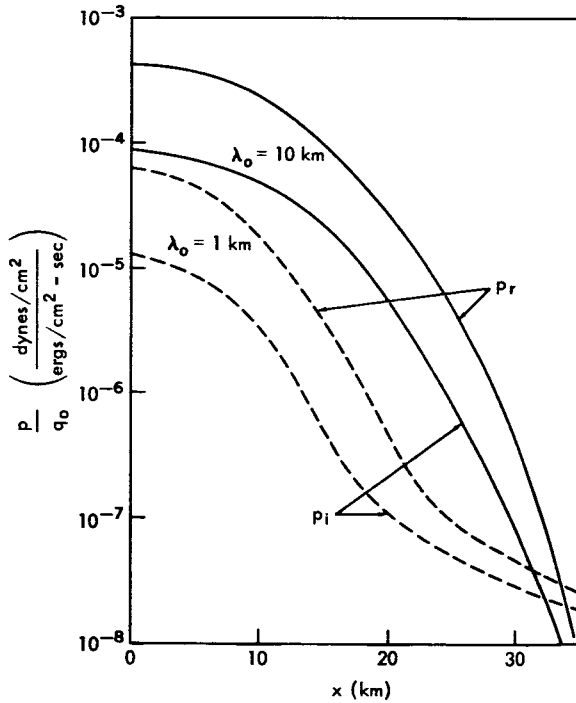


Figure 5—A plot of the intensity of the cellular waves $p_r$ and $p_i$ on the ground, as a function of the input energy flux $q_0$ for $\tau = 30$ sec and $h = H$, vs. $x$, the horizontal distance from the center of the source. Full lines and dashed lines correspond to $\lambda_0 = 10$ km and $\lambda_0 = 1$ km, respectively.
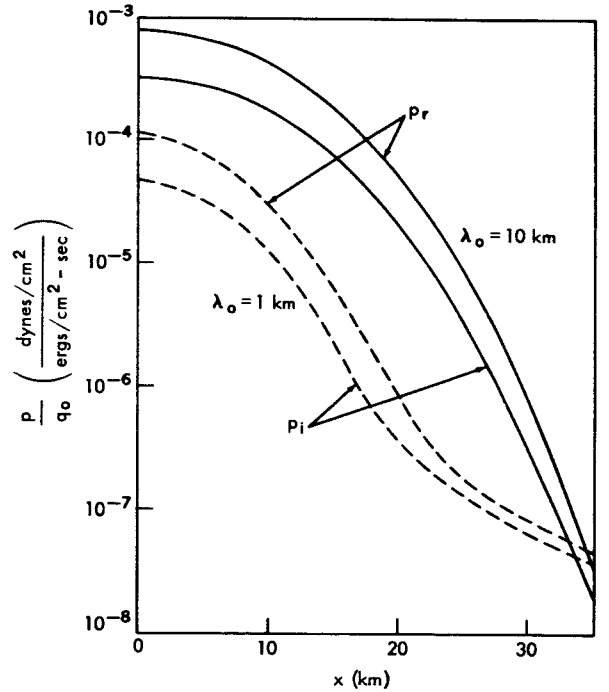


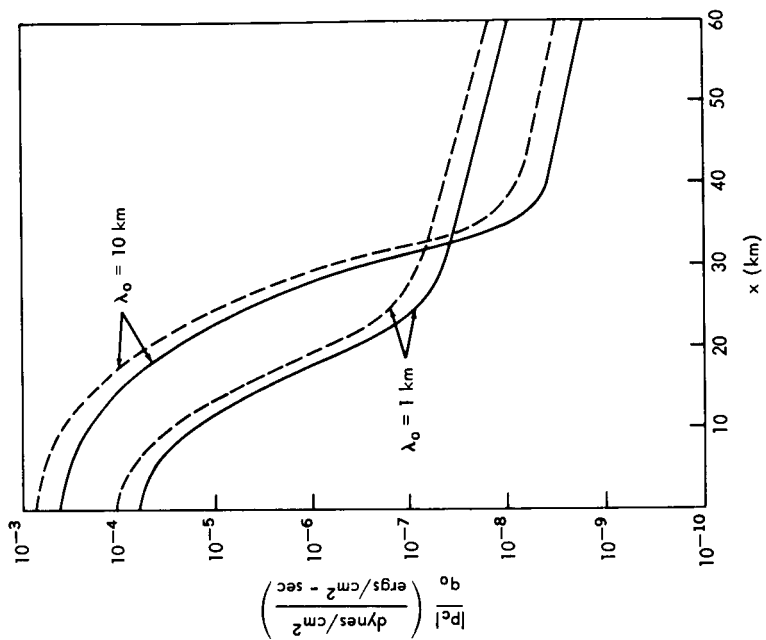Figure 6—The same plot as Figure 5 except that $h = 1/2H$ instead of $h = H$.

Figure 8—The same plot as Figure 7 except that $\tau = 30$ sec.



Figure 7—A plot of the intensity of cellular waves produced by periodic auroral heating, $|p_c| = \sqrt{p_r^2 + p_i^2}$, vs. the horizontal distance from the center of the source for $\tau = 10$ sec. Full lines and dashed lines stand for $h = H$ and $h = 1/2H$, respectively.
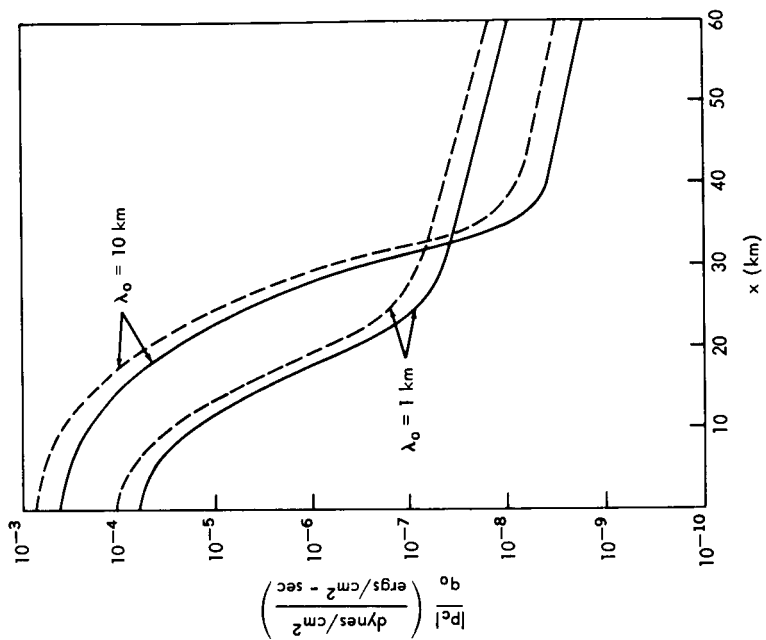
## ATTENUATION

Because of the viscosity and thermal conductivity of air, acoustic waves in the atmosphere attenuate. The attenuation coefficient $\alpha(\tau)$, in $cm^{-1}$, for a wave of period $\tau$ is given approximately by (Reference 48)

$$\alpha(\tau) = \frac{4\pi^2}{\tau^2} \frac{1}{c^3} \left( \frac{4}{3} \nu + \frac{\gamma-1}{\gamma} a^2 \right) \quad , \quad (69)$$

where the coefficient of kinematic viscosity $\nu$ is approximately

$$\nu = \frac{1.7 \times 10^{-4}}{\rho(z)} \quad (70)$$

in $cm^2/sec$, and the coefficient of thermal conductivity $a^2$ is

$$a^2 = \frac{2.1 \times 10^{-5}}{\rho(z)} \quad , \quad (71)$$

in $cm^2/sec$.



Figure 9—The same plot as Figure 7 except that $\tau = 100$ sec.

Since the air density $\rho$ decreases exponentially with height, $a^2$ and $\nu$ increase exponentially with altitude. The so-called attenuation factor,

$$f_a (\tau, z) = \exp \left[ - \int_0^z \alpha(\tau, z') dz' \right] , \quad (72)$$

is shown in Figure 11 as a function of height, for $\tau = 10$ sec, 30 sec, and 100 sec.

It should be noted that the relative amplitude of the pressure wave grows as it propagates upward by a factor $e^{z/2H}$, where H is the scale height, whereas the absolute amplitude decreases by a factor $e^{-z/2H}$, because of the exponential decrease of air density (Reference 49). Therefore, if the amount of excitation energy is the same, the absolute intensity of the pressure wave at the ground increases with the base of the excitation level. This is shown by Equation 29 and Equations C9 and C10 with a factor $e^{z_0/2H}$ for $p_s$, $p_c$ ($z = 0$), and $p_{nc}$ ($z = 0$), and by a curved dash line in Figure 11.

However, because of the steep increase of the kinematic viscosity of air with altitude, the yield of pressure wave excitation drops sharply above a certain altitude for a given period (or frequency) of the wave. This is shown in Figure 12 for wave periods of $\tau = 10$, 30, and 100 sec.
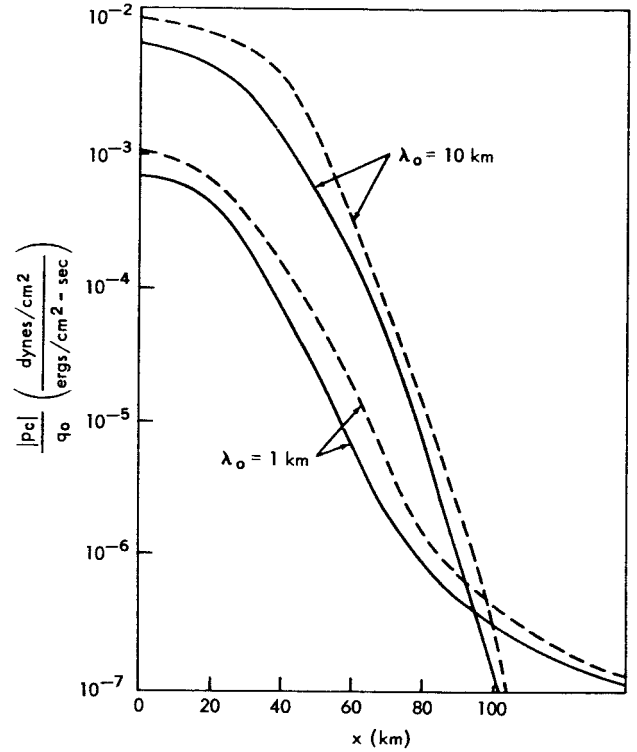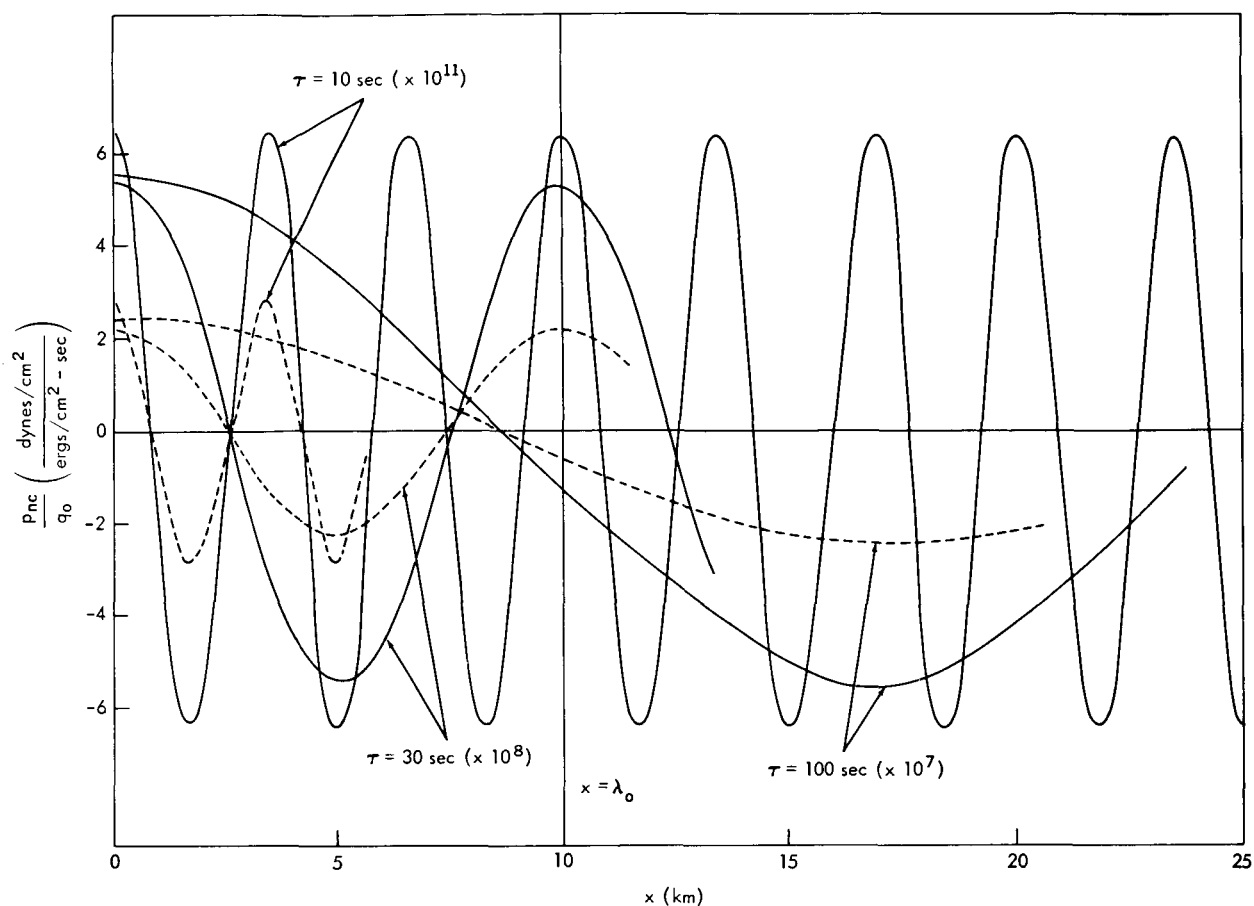
Figure 10—Intensity distribution of noncellular waves on the ground, $p_{nc}$, in the units of $q_0$, vs. horizontal distance x from the center of the source of width $\lambda_0 = 10$ km. Notice that the vertical scales are magnified by a factor attached to each curve. Full lines and dashed lines stand for $h = H$ and $h = 1/2H$, respectively.

Table 1

Intensity of the Cellular Mode of Infrasonic Waves on the Ground Below the Center of the Source in Units of $q_0$.

| h = H | $p_r$ | $p_i$ | $|p_c|$ | h = 1/2H | $p_r$ | $p_i$ | $|p_c|$ |
|---|---|---|---|---|---|---|---|
| $\lambda_0 = 1$ km | | | | $\lambda_0 = 1$ km | | | |
| $\tau = 10$ sec. | $6.74 \times 10^{-6}$ | $4.40 \times 10^{-7}$ | $6.75 \times 10^{-6}$ | $\tau = 10$ sec. | $1.33 \times 10^{-5}$ | $1.79 \times 10^{-6}$ | $1.34 \times 10^{-5}$ |
| 30 sec. | $6.15 \times 10^{-5}$ | $1.21 \times 10^{-5}$ | $6.28 \times 10^{-5}$ | 30 sec. | $1.10 \times 10^{-4}$ | $4.79 \times 10^{-5}$ | $1.23 \times 10^{-4}$ |
| 100 sec. | $5.46 \times 10^{-4}$ | $4.26 \times 10^{-4}$ | $6.92 \times 10^{-4}$ | 100 sec. | $2.77 \times 10^{-4}$ | $1.02 \times 10^{-3}$ | $1.06 \times 10^{-3}$ |
| $\lambda_0 = 10$ km | | | | $\lambda_0 = 10$ km | | | |
| $\tau = 10$ sec. | $1.82 \times 10^{-5}$ | $1.20 \times 10^{-6}$ | $1.83 \times 10^{-5}$ | $\tau = 10$ sec. | $3.62 \times 10^{-5}$ | $4.80 \times 10^{-6}$ | $3.65 \times 10^{-5}$ |
| 30 sec. | $4.29 \times 10^{-4}$ | $8.57 \times 10^{-5}$ | $4.38 \times 10^{-4}$ | 30 sec. | $7.91 \times 10^{-4}$ | $3.32 \times 10^{-4}$ | $8.58 \times 10^{-4}$ |
| 100 sec. | $5.25 \times 10^{-3}$ | $4.11 \times 10^{-3}$ | $6.67 \times 10^{-3}$ | 100 sec. | $2.68 \times 10^{-3}$ | $9.85 \times 10^{-3}$ | $1.02 \times 10^{-2}$ |
| $\lambda_0 = 100$ km | | | | $\lambda_0 = 100$ km | | | |
| $\tau = 10$ sec. | $1.82 \times 10^{-5}$ | $1.20 \times 10^{-6}$ | $1.83 \times 10^{-5}$ | $\tau = 10$ sec. | $3.62 \times 10^{-5}$ | $4.80 \times 10^{-6}$ | $3.65 \times 10^{-5}$ |
| 30 sec. | $4.84 \times 10^{-4}$ | $1.01 \times 10^{-4}$ | $4.94 \times 10^{-4}$ | 30 sec. | $8.92 \times 10^{-4}$ | $3.73 \times 10^{-4}$ | $9.68 \times 10^{-4}$ |
| 100 sec. | $1.43 \times 10^{-2}$ | $1.14 \times 10^{-2}$ | $1.83 \times 10^{-2}$ | 100 sec. | $7.62 \times 10^{-3}$ | $2.72 \times 10^{-2}$ | $2.83 \times 10^{-2}$ |

Table 2

Values for $p_{nc}$, $p_{nc}/|p_c|$, and $x_0$, the Horizontal Distance of the first Nodal Lines from the Center of the Source (horizontal width assumed to be $\lambda_0 = 10$ km).

| h = H | $p_{nc}$ | $p_{nc}/|p_c|$ | $x_0$ (km) | h = 1/2H | $p_{nc}$ | $p_{nc}/|p_c|$ | $x_0$ (km) |
|---|---|---|---|---|---|---|---|
| $\tau$ = 10 sec | $1.28 \times 10^{-9}$ | $7.0 \times 10^{-5}$ | 0.85 | $\tau$ = 10 sec | $1.11 \times 10^{-9}$ | $3.03 \times 10^{-5}$ | 0.85 |
| 30 sec | $3.24 \times 10^{-8}$ | $7.4 \times 10^{-5}$ | 2.56 | 30 sec | $2.73 \times 10^{-8}$ | $3.18 \times 10^{-5}$ | 2.56 |
| 100 sec | $1.10 \times 10^{-5}$ | $1.66 \times 10^{-3}$ | 8.31 | 100 sec | $1.02 \times 10^{-5}$ | $9.8 \times 10^{-4}$ | 8.30 |

It can be seen that there is an effective height of excitation of atmospheric acoustic waves for a given period and that this height increases with the period.

As mentioned in the introduction, the excitation of pressure waves by hydromagnetic waves is only effective above the height of auroral activities. Figure 12 shows that waves produced at such a height are greatly attenuated before they reach the ground. Therefore, the contribution of hydromagnetic waves to the excitation of
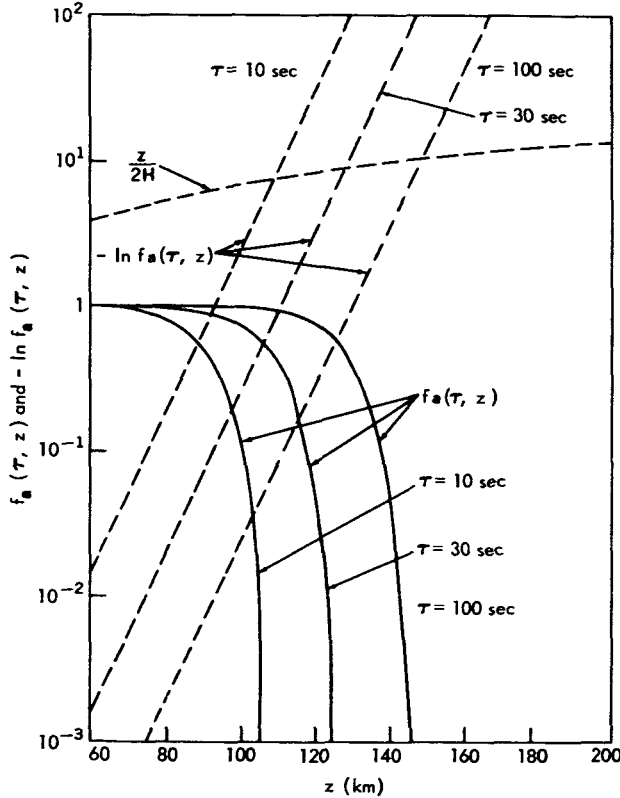
Figure 11—Attenuation factor $f_a$ $(\tau, z)$ vs. altitude of the source z in km and $-\ln f_a$ $(\tau, z)$ vs. z:

$$-\ln f_a(\tau, z) = \int_0^z \alpha(\tau, z') \, dz',$$

a dashed line is also used to indicate the exponential amplification factor $\ln (\rho_z \, \rho_0)^{1/2} \approx z/2H$, where the scale height H is assumed to be 8 km.
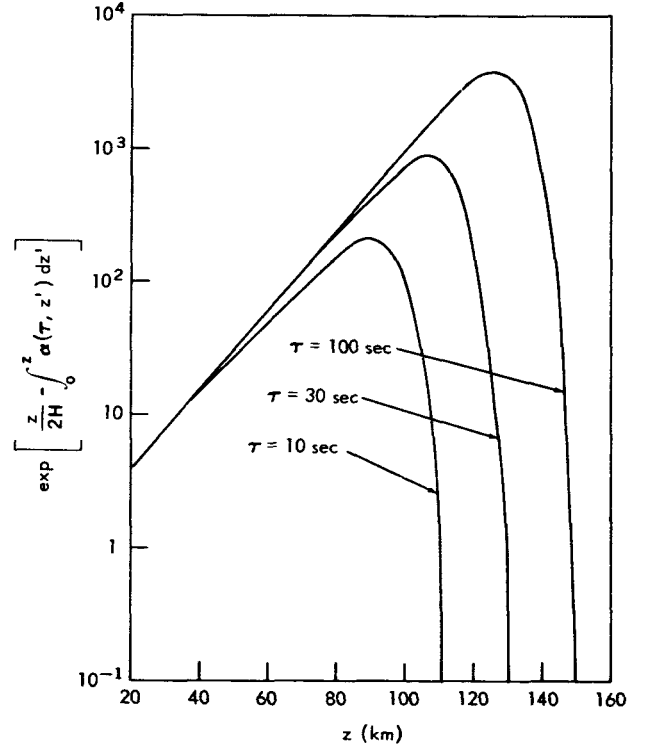
Figure 12—Relative yield of the source to the infrasonic waves in the isothermal atmosphere

$$\sqrt{\frac{\rho(z)}{\rho_0}} \, f_a(\tau, z) \approx \exp\left[\frac{z}{2H} - \int_0^z \alpha(\tau, z') \, dz'\right]$$

vs. the altitude of the source z, where the scale height H is assumed to be 8 km.

internal atmospheric waves is practically negligible. A more quantitative discussion will be given in the next section.

## CONDITIONS FOR WAVE FORMATION

According to previous calculations, a pressure variation at the ground of the order of 1 dyne/cm² can be expected if the maximum rate of heat generation is of the order of 100 ergs/cm²-sec and the layer of periodic heating is around 100 km altitude, with a thickness less than 10 km. Electrons with an energy of the order of 100 kev will lose most of their energy within a layer of the order of 10 km thickness around the height of 100 km (Reference 19, p. 290). According to Chamberlain, the rate of heat generation is the order of 60 ergs/cm²-sec in a bright aurora. Therefore, if the rate of heat generation changes periodically with this order of amplitude, barometric oscillations of the order of 1 dyne/cm² at sea level can be expected from the sources in the upper atmosphere.

However, several other conditions must be satisfied in order that the energy brought into the upper air by auroral electrons can be converted efficiently to pressure waves in the atmosphere. At first, the time $\tau_1$, in which an electron arrives at auroral height from outer space, should be smaller than the period, $\tau$, of the waves concerned. If $\tau_1 \gg \tau$, the phase of the time variation of the source differs from place to place, and the resultant pressure wave originating from those different sources is weakened by superposition.

Since the auroral electrons, whose velocity is of the order of $10^9$ cm/sec, lose their energy within a layer of 10 km thickness, $\tau_1 <$ approx. $10^{-4}$ sec. This is much smaller than the period of the acoustic waves considered here.

As discussed by Hanson and Johnson (Reference 50), electrons impinging into the upper atmosphere lose their energy mostly by inelastic collisions with neutral air particles until $\approx 2$ ev, which is the lowest excitation energy of atomic oxygen ($^1D$ state). The time $\tau_2$ for $^1D$ excitation collisions with oxygen atoms is of the order of $10^{-3}$ sec at 100 km and of the order of 1 sec at 400 km.

Below 2 ev, the electrons lose energy in the upper atmosphere mainly by elastic collisions with ambient electrons. The time for those low energy electrons to equilibrate with ambient electrons, $\tau_3$, is obtained from the expression for the rate of energy loss of a fast electron immersed in a thermalized plasma (Reference 50),

$$\tau_3 \approx \frac{5.7 \times 10^3 \, E^{3/2}}{N_e} , \tag{73}$$

where $E$ is the electron energy, i.e., $E \approx 2$ ev, and $N_e$ is the electron concentration in $cm^{-3}$. The equilibration time, $\tau_3$, given by this expression is about $10^{-1}$ sec at 100 km and of the order of $10^{-2}$ sec above 350 km. Thus $\tau_2 + \tau_3$ is much smaller than the periods of the acoustic waves under discussion.

It should be noted that elastic collisions with neutral particles dominate over those with ambient electrons below the F2 maximum (around 300 km). The time constant $\tau_4$ for these elastic collisions consists of $\tau(O)$ and $\tau N_2$, the time constants for the loss of excess electron energy to atomic oxygen and to molecular nitrogen, respectively (Reference 50), and is given by

$$\tau_4 = \frac{2.08 \times 10^{11} E^{-1/2}}{n(O) + 2.36n(N_2)}, \tag{74}$$

where $n(O)$ and $n(N_2)$ are the concentration per cm$^3$ of atomic oxygen and of molecular nitrogen, respectively. For E = 2 ev, $\tau_4$ is of the order of 0.1 sec at 100 km and increases with height. It is of the order of 100 sec at 350 km.

As shown in the previous section, the excitation of atmospheric pressure waves above 200 km is not important; the time constant $\tau_4$ does not destroy the condition of wave formation. In other words, below 200 km $\tau_1 + \tau_2 + \tau_3 + \tau_4 < $ approx. $\tau$.

Another condition necessary for wave formation is that the time constant for cooling in a certain domain of auroral activity must be much longer than the period of oscillation. If the initial temperature $T_0$ is assumed to be horizontally uniform within the domain of the source, $-\lambda_0 \leq x \leq \lambda_0$, then the temperature at the center after t (sec) is

$$T(t) = (T_0 - T_a) \Phi\left(\frac{\lambda_0}{2\sqrt{a^2 t}}\right), \tag{75}$$

where

$$\Phi(y) = \frac{2}{\sqrt{\pi}} \int_0^y e^{-x^2} dx, \tag{76}$$

and $a^2$ is the thermal diffusivity (coefficient of thermal conduction) of air. $T_a$ is the temperature outside the source.

The time, $t_a$, necessary to reduce the initial temperature difference between the inside and outside of the source region can be estimated from

$$\left.\begin{aligned} \Phi\left(\frac{\lambda_0}{2\sqrt{a^2 t_a}}\right) &= \frac{1}{2}, \\ t_a &\approx \frac{\lambda_0^2}{a^2}. \end{aligned}\right\} \tag{77}$$

Since the thermal diffusivity of air $a^2$ at a height of 100 km is of the order of $10^6$ cm$^2$/sec (see Equation 71), the minimum source width necessary to satisfy the condition for thermal oscillation is of the order of 30m for a period of 10 sec, and of the order of 100m for a period of 100 sec. The source width considered in the present calculation is significantly larger than

these widths. In other words, the time constant for source cooling is sufficiently long for pressure wave production.

## OTHER POSSIBLE MECHANISMS

Now the possibility of other suitable mechanisms for the generation of microbarometric oscillations during magnetic disturbances will be considered.

### Periodic Heating Due to the Absorption of Hydromagnetic Waves

As stated in the introduction, hydromagnetic waves from the magnetosphere lose part of their energy in the lower exosphere and in the ionosphere. The remaining energy, which leaks through the ionosphere, is observed as fluctuations of the geomagnetic field intensity or geomagnetic pulsations.

The rate of energy dissipation of hydromagnetic waves in the ionosphere increases with increasing frequency (References 6, 51, and 52). According to Watanabe, the dissipation of the hydromagnetic wave energy in the ionosphere is negligible for waves with periods longer than 20 sec. In the auroral region, the amplitude of geomagnetic pulsations sometimes exceeds several tens of gammas (i.e., giant pulsations) and the periods are sometimes longer than several tens of seconds. The intensity of the incident wave is usually smaller for higher frequencies (Reference 15). As shown by the power density of the small scale fluctuations of magnetic field intensity observed in the earth's magnetosphere between 5 and 15 earth radii (Reference 3), the frequency spectrum of hydromagnetic waves, which are regarded as the origins of geomagnetic pulsations observed at the earth's surface, is a decreasing function of frequency above the ionosphere. In any case, the upper limit of the incident wave amplitude may be taken as $100\,\gamma$. The energy flux associated with these hydromagnetic waves is then of the order of several ergs/cm$^2$-sec$^1$, under the assumption that the Alfvén wave velocity above the ionosphere is of the order of $10^8$ cm/sec. The rate of heat generation by absorption of these hydromagnetic waves in the upper ionosphere has been estimated by several authors and their results are shown in Table 3.

Table 3

Rate of Heat Generation Due to Attenuation of Hydromagnetic Waves with a $100\,\gamma$ Incident Amplitude.

| Source | Period of HM waves (sec) | Rate of Heat Generation in an Air Column of unit cross section (erg/cm$^2$-sec) | Thickness of Heating Layer (km) | Altitude of the Center of the Heat Generating Layer (km) |
|---|---|---|---|---|
| Dessler (Reference 53) | 1 | 1.3 | 100 | 170 |
| Francis and Karplus (Reference 51) | 6.3<br>0.3 | 0.7<br>1.6 | 50<br>100 | 125<br>180 |
| Akasofu (Reference 52) | 1<br>10<br>100 | 9.7<br>0.17<br>0.028 | 100<br>200<br>300 | 225<br>240<br>250 |

The rate of heat generation is generally less than 1 erg/cm²-sec, except when the period is 1 sec. Therefore the amount of heat generated by hydromagnetic waves penetrating the ionosphere is smaller than that due to the auroral particles. Table 3 also contains estimates of the thickness of the layer of heat generation. In every case the thickness is much larger for hydromagnetic waves than for auroral particles.

As shown in Figure 12, the effective height of pressure wave generation by periodic heating of the upper air is limited, and it is lower for the shorter period. Therefore, generation of acoustic waves by the attenuation of hydromagnetic waves is less efficient than generation by the periodic heating due to auroral particles, even if the energy flux of the incident wave is increased to be the same as the latter.

## Pressure Waves Due to the Impacts of Auroral Particles

A particle coming into the atmosphere loses its energy by transferring its downward momentum to the air particles. A pressure wave can be generated if the flux of the particle changes periodically with time.

The upper limit of the pressure intensity, from this process, can be estimated by assuming that all the incoming particles would stop in a very short time within a very thin layer. By assuming the average energy of incident electrons is 6 kev and the maximum flux is of the order of $10^{10}$ cm$^{-2}$-sec$^{-1}$, the maximum pressure exerted upon the thin layer of virtual shock absorber is estimated to be of the order of $4.10^{-8}$ dynes/cm². The corresponding intensity at the earth's surface is of the order of $10^{-5}$ dyne/cm², if all electrons stop at an altitude of 100 km.

## Penetration of Hydromagnetic Waves Through the Ionosphere

As mentioned above, most geomagnetic pulsations are due to hydromagnetic oscillations in the exosphere. These oscillations are related to electromagnetic oscillations in the space between the earth's surface and the lower boundary of the ionosphere. Any oscillation mode in which the compression of atmospheric matter is involved gives rise to a variation in the density, and consequently a pressure variation. Therefore, it may be possible that geomagnetic pulsations and microbarometric oscillations have the same origin, i.e., hydromagnetic oscillations of the earth's exosphere.

A simple situation can be found at the geomagnetic equator, where geomagnetic pulsations appear sometimes in the N-S component of the geomagnetic field, with amplitudes of the order of several tens of gammas and periods of several minutes (Reference 54). The origins of this kind of pulsation presumably exist in the outer boundary of earth's magnetosphere near the geomagnetic equatorial plane, and it may be propagated as a modified Alfvèn wave. A modified Alfvèn wave is a transverse wave with respect to changes in the electric and magnetic fields. On the other hand, it is a longitudinal wave when viewed as fluid motion (Reference 55). An electromagnetic wave as well as a pressure wave should be in the space between the earth's surface and the lower boundary of the ionosphere. The energy flux associated with an incident modified Alfvèn wave is

roughly $\left(B^2/8\pi\right) V_A$, where $V_A$ is the group velocity of the modified Alfvèn waves and can be taken as the Alfvèn wave velocity at a higher portion of the ionosphere. $B$ is the amplitude of the wave, i.e., the intensity of magnetic fluctuation above the ionosphere.

By assuming conservation of energy flux, the upper limit of the amplitude of the pressure wave at the earth's surface, $p_e$, can be estimated as follows:

$$\frac{1}{2} \frac{p_e^2}{c_s \rho_s} = \frac{B^2}{8\pi} V_A \quad ,$$

where $c_s$ is the sound wave velocity at the earth's surface, and $\rho_s$ is the air density at the earth's surface. By taking $V_A = 3.10^7$ cm/sec (corresponding to daytime at the sunspot maximum activity) $B = 30\gamma$, $c_s = 3.10^4$ cm/sec, and $\rho_s = 1.25 \times 10^{-3}$ gm/cm³, we find $p_e \approx 3$ dynes/cm². In this estimate the conversion factor between the energy of incident Alfvèn waves and that of secondary pressure waves is assumed to be unity. This factor must actually be very small because of reflections and energy dissipations of incident waves at the upper part of the ionosphere. If it is not small, infrasonic waves could appear in the equatorial region during strong magnetic disturbances. Since the occurrence of aurorae in these regions is negligible, this might provide a method of direct detection of modified Alfvèn waves coming into the earth's atmosphere from the magnetosphere.

## CONCLUSIONS

We have shown that one of the most plausible mechanisms for pressure wave generation during geomagnetic disturbances is the periodic heating of the polar ionosphere by auroral particles, observed as pulsating aurorae. As emphasized by Campbell (Reference 56) the main energy source for this type of auroral activity is not necessarily incident auroral particles, but a flow of secondary electrons called the electro-jet. In this respect periodic heating by these intermittent electric currents is essentially the same as the so-called Joule heating discussed by Cole (References 57 and 58).

The following conclusions can be drawn from the present calculation:

1. From Figures 3, 5-9, and 13 it can be seen that an incident energy flux of more than 100 ergs/cm²-sec will produce acoustic waves observable at the ground, provided the periods are longer than about 10 seconds.

2. The relative intensity of the pressure wave at the ground is higher when the heating is concentrated within a thin layer than when it is distributed over a wide range of altitudes (Figures 3, 5, and 6).

3. The intensity ratio between the inside of the source region and the outside is smaller for long periods than for short periods, as expected.

4. The gradient of intensity around the boundary of the source is steeper when the width of the source is wide.

5. Inside the source the ratio of non-cellular to cellular wave intensity is of the order of $10^{-5}$ for $\tau = 10$ sec and $10^{-3}$ for $\tau = 100$ sec. Although the noncellular intensity exceeds the cellular at large distances from the source, the contribution of the non-cellular wave to the observed intensity is negligible, because both waves attenuate in long distance propagation.

6. According to the present calculations, which are based on an isothermal atmosphere, the intensity of acoustic waves more than several hundred km from the region of auroral activity is negligible. For the real atmosphere, therefore, the horizontal propagation of acoustic waves through the ducts around the mesopause and the stratopause is rather important in explaining the diurnal variation of the arrival direction of these waves during the period of high geomagnetic activity, as shown in Figure 1.

7. It should be noted that auroral activities are not necessarily within the auroral zone but, rather, extend toward lower latitudes (nearly to 50°N), when these sonic waves are observed during the periods of magnetic disturbances (as can be seen from the auroral visoplot shown in Figure 2).
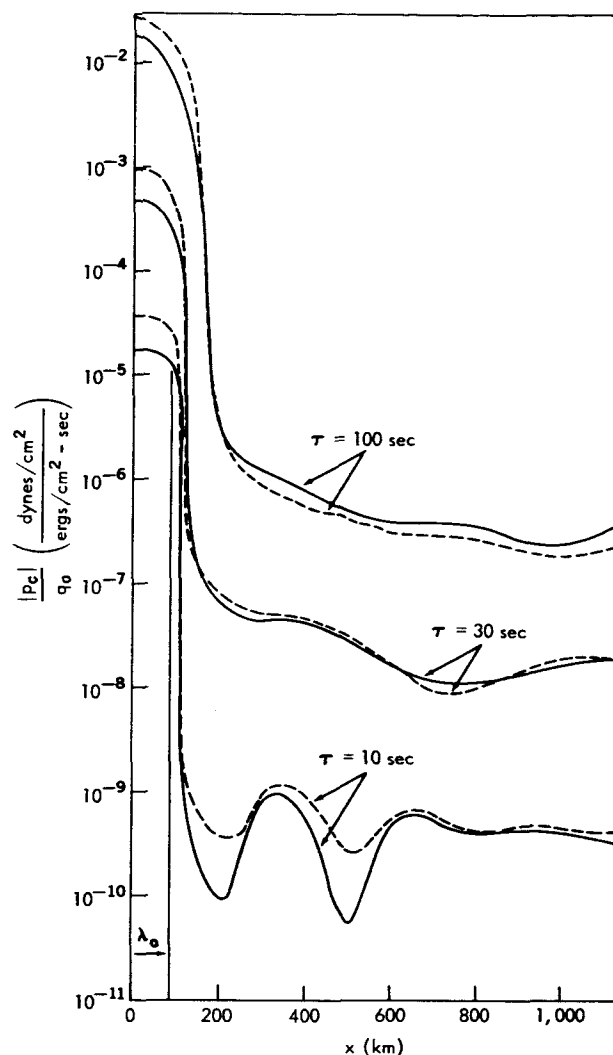
Figure 13—Intensities of cellular waves on the ground in the units of $q_0$ vs. the horizontal distance x from the center of the source, of which the width $\lambda_0$ is 100 km, for $\tau = 10$ sec, 30 sec and 100 sec. Full lines and dashed lines stand for h = H and h = 1/2H, respectively.

To show the position and structure of sonic ducts as well as attenuation of the waves requires the actual atmospheric temperature distributions. This is discussed elsewhere (Reference 59).

Finally, it should be noted that the energy flux of acoustic waves at the ground S in ergs/cm$^2$-sec is

$$S = Ec ,$$ (78)

where

$$E = \frac{p_s^2}{2\rho_s c^2} \; ; \tag{79}$$

$p_s$ and $\rho_s$ are the maximum amplitude of pressure change in dynes/cm² and the static density of air at sea level, and c is the sound velocity in cm/sec.

Since $\rho_s$ is of the order of $1.25 \times 10^{-3}$ gm/cm³, the energy flux corresponding to $p_s = 1$ dyne/cm² is approximately $1.4 \times 10^{-2}$ erg/cm²-sec. To show the energy relation between the input power and the observed output intensity, as given in Figures 3, 5-10, and 13, the above relation must be used.

## ACKNOWLEDGMENTS

REFERENCES

1. Chrzanowski, P., Green, G., Lemmon, K. T., and Young, J. M., "Traveling Pressure Waves Associated with Geomagnetic Activity," *J. Geophys. Res.* 66(11):3727-3733, November 1961.

2. Campbell, W. H., "Natural Electromagnetic Energy Below the ELF Range," *Nat. Bur. Stand. J. Res.* 64D(4):409-411, July-August 1960.

3. Sonett, C. P., Judge, D. L., Sims, A. R., and Kelso, J. M., "A Radial Rocket Survey of the Distant Geomagnetic Field," *J. Geophys. Res.* 65(1):55-68, January 1960.

4. Heppner, J. P., Ness, N. F., Scearce, C. S., and Skillman, T. L., "Explorer 10 Magnetic Field Measurements," *J. Geophys. Res.* 68(1):1-46, January 1, 1963.

5. Heppner, J. P., Ness, N. F., Skillman, T. L., and Scearce, C. S., "Magnetic Field Measurements with the Explorer X Satellite," in: *Goddard Space Flight Center Contributions to the 1961 Kyoto Conf. on Cosmic Rays and the Earth Storm,* ed. by F. B. McDonald, NASA Technical Note D-1061, June 1962, pp. 1-20.

6. Watanabe, T., "Electrodynamical Behaviour and Screening Effect of the Ionosphere," *Sci. Rept. Tohoku Univ.* Ser. 5, 9:81-98, 1957.

7. Watanabe, T., "Law of Electric Conduction for Waves in the Ionosphere," *J. Atmos. Terres. Phys.* 24:117-125, February 1962.

8. Piddington, J. H., "The Transmission of Geomagnetic Disturbances Through the Atmosphere and Interplanetary Space," *Geophys. J.* 2(3):173-189, September 1959.

9. Scholte, J. G., and Veldkap, J., "Geomagnetic and Geoelectric Variations," *J. Atmos. Terres. Phys.* 6(1):33-45, January 1955.

10. Dungey, J. W., "The Propagation of Alfvèn Waves Through the Ionosphere," Penn. State Univ. Sci. Rept. 57, 1954.

11. Kato, Y., and Watanabe, T., "Further Study on the Cause of Giant Pulsations," *Sci. Rept. Tohoku Univ.* Ser. 5, 8:1-10, 1956.

12. Obayashi, T., and Jacobs, J. A., "Geomagnetic Pulsations and the Earth's Outer Atmosphere," *Geophys. J.* 1(1):53-63, March 1958.

13. Obayashi, T., "Geomagnetic Storms and the Earth's Outer Atmosphere," *Rept. Ionosphere Res. Japan* 12(3):301-335, September 1958.

14. Dessler, A. J., "The Propagation Velocity of World-Wide Sudden Commencements of Magnetic Storms," *J. Geophys. Res.* 63(2):405-408, June 1958.

15. Jacobs, J. A., and Watanabe, T., "Propagation of Hydromagnetic Waves in the Lower Exosphere and the Origin of Short Period Geomagnetic Pulsations," *J. Atmos. Terres. Phys.* 24:413-434, June 1962.

16. Heppner, J. P., "A Study of Relationships Between the Aurora Borealis and the Geomagnetic Disturbances Caused By Electric Currents in the Ionosphere," Canad. Defense Res. Board Rept. DR-135, 1958.

17. Campbell, W. H., and Rees, M. H., "A Study of Auroral Coruscations," *J. Geophys. Res.* 66(1):41-55, January 1961.

18. McIlwain, C. E., "Direct Measurement of Particles Producing Visible Auroras," *J. Geophys. Res.* 65(9):2727-2747, September 1960.

19. Chamberlain, J. W., "Physics of the Aurora and Airglow," New York: Academic Press, 1961.

20. Lamb, H., "Hydrodynamics," 6th ed., Cambridge, England: The University Press, 1932.

21. Bjerknes, V. F. K., Bjerknes, J., Solberg, H., and Bergeron, T., "Physikalische Hydrodynamik," Berlin: J. Springer, 1933.

22. Wilkes, M. V., "Oscillations of the Earth's Atmosphere," Cambridge, England: The University Press, 1949.

23. Wilkes, M. V., "The Thermal Excitation of Atmospheric Oscillations," *Roy. Soc. Proc.* A207:358-370, July 6, 1951.

24. Sawada, R., "On the Role of Thermal Excitation in the Atmospheric Tides," *Geophys. Mag.* 26(4):267-281, August 1955.

25. Taylor, G. I., "Waves and Tides in the Atmosphere," *Roy. Soc. Proc.* A126:169-183, December 2, 1929.

26. Pekeris, C. L., "The Propagation of a Pulse in the Atmosphere," *Roy. Soc. Proc.* A171:434-449, July 7, 1939.

27. Pekeris, C. L., "The Propagation of a Pulse in the Atmosphere. II," *Phys. Rev.* 73:145-154, January 15, 1948.

28. Scorer, R. S., "The Dispersion of a Pressure Pulse in the Atmosphere," *Roy. Soc. Proc.* A201:175-186, March 22, 1950.

29. Gossard, E. E., and Munk, W., "On Gravity Waves in the Atmosphere," *J. Met.* 11:259-269, 1954.

30. Gossard, E. E., "Vertical Flux of Energy into the Lower Ionosphere from Internal Gravity Waves Generated in the Troposphere," *J. Geophys. Res.* 67(2):745-757, February 1962.

31. Yamamoto, R., "Study of the Microbarographic Waves (I), Theory of the Microbarographic Waves (I)," *Met. Soc. Japan J.* 34:235-243, December 1956.

32. Yamamoto, R., "A Study of Microbarographic Waves (II), Theory of the Microbarographic Waves (II) (continued), *Met. Soc. Japan J.* 35:321-326, 1957.

33. Press, F., and Harkrider, D., "Propagation of Acoustic-Gravity Waves in the Atmosphere," *J. Geophys. Res.* 67(10):3889-3908, September 1962.

34. Weston, V. H., "The Pressure Pulse Produced by a Large Explosion in the Atmosphere," *Canad. J. Phys.* 39(7):993-1009, July 1961.

35. Weston, V. H., "The Pressure Pulse Produced by a Large Explosion in the Atmosphere. II," *Canad. J. Phys.* 40(4):431-445, April 1962.

36. Weston, V. H., "Gravity and Acoustical Waves," *Canad. J. Phys.* 40(4):446-453, April 1962.

37. Martyn, D. F., "Cellular Atmospheric Waves in the Ionosphere and Troposphere," *Roy. Soc. Proc.* A201:216-234, March 22, 1950.

38. Sen, H. K., and White, M. L., "Thermal and Gravitational Excitation of Atmospheric Oscillations," *J. Geophys. Res.* 60(4):483-495, December 1955.

39. White, M. L., "Gravitational and Thermal Oscillations in the Earth's Upper Atmosphere," *J. Geophys. Res.* 61(3):489-499, September 1956.

40. White, M. L., "Thermal and Gravitational Atmospheric Oscillations — Ionospheric Dynamo Effects Included," *J. Atmos. Terres. Phys.* 17(3):220-245, February 1960.

41. Hines, C. O., "Hydromagnetic Resonance in Ionospheric Waves," *J. Atmos. Terres. Phys.* 7(1-2):14-30, August 1955.

42. Hines, C. O., "Internal Atmospheric Gravity Waves at Ionospheric Heights," *Canad. J. Phys.* 38(11):1441-1481, November 1960.

43. Eckart, C., "The Thermodynamics of Irreversible Processes. I. The Simple Fluid," *Phys. Rev.* 58(3):267-269, August 1, 1940.

44. Eckart, C., "The Thermodynamics of Irreversible Processes. II. Fluid Mixtures," *Phys. Rev.* 58(3):269-275, August 1, 1940.

45. Eckart, C., and Ferris, H. G., "Equations of Motion of the Ocean and Atmosphere," *Rev. Mod. Phys.* 28(1):48-52, January 1956.

46. Eckart, C., "Hydrodynamics of Oceans and Atmospheres," New York: Pergamon Press, 1960.

47. Tolstoy, I., "The Theory of Waves in Stratified Fluids Including the Effects of Gravity and Rotation," *Rev. Mod. Phys.* 35(1):207-230, January 1963.

48. Rayleigh, J. W. S., "The Theory of Sound, Vol. II, Cambridge Trans," 1929, p. 315.

49. Schrödinger, E., "Zur Akustik der Atmosphäre," *Phys. Zeits.* 18:445-453, October 1, 1917.

50. Hanson, W. B., and Johnson, F. S., "Electron Temperature in the Ionosphere," *Mem. Roy. Soc. Sci. Liege* 4:390-423, 1960.

51. Francis, W. E., and Karplus, R., "Hydromagnetic Waves in the Ionosphere," *J. Geophys. Res.* 65(11):3593-3600, November 1960.

52. Akasofu, S., "On the Ionospheric Heating by Hydromagnetic Waves Connected with Geomagnetic Micropulsations," *J. Atmos. Terres. Phys.* 18(2-3):160-173, June 1960.

53. Dessler, A. J., "Ionospheric Heating by Hydromagnetic Waves," *J. Geophys. Res.* 64(4):397-401, April 1959.

54. Matsuura, N., and Nagata, T., "Turbulence in the Upper Atmosphere," *Rept. Ionosphere Res. Japan,* 12:147-149, 1958.

55. van de Hulst, H. C., "Interstellar Polarization and Magneto-Hydrodynamic Waves," in: *Problems of Cosmical Aerodynamics, Proceedings of the Symposium on the Motion of Gaseous Masses of Cosmical Dimensions,* Paris: August 16-18, 1949, Dayton, Ohio: Central Air Documents Office, 1951, pp. 45-56.

56. Campbell, W. H., "Theory of Geomagnetic Micropulsations," AGU annual meeting at Washington, D. C., April 28, 1962.

57. Cole, K. D., "A Source of Energy for the Ionosphere," *Nature* 194:75, April 7, 1962.

58. Cole, K. D., "Atmospheric Blow-Up at the Auroral Zone," *Nature* 194:761, May 26, 1962.

59. Maeda, K., "Acoustic Heating of the Polar Night Mesosphere," NASA Technical Note D-1912, November 1963.

# Appendix A

## Derivation of Differential Equation 37

By differentiating Equations 30 and 31 with respect to $t$ and using Equation 33

$$\frac{\partial^2 u}{\partial t^2} = \frac{\partial}{\partial x}\left(c^2 \chi - gw\right) - \frac{1}{\rho_0}\frac{\partial s}{\partial x} \quad . \tag{A1}$$

$$\frac{\partial^2 w}{\partial t^2} = \frac{\partial}{\partial z}\left(c^2 \chi - gw\right) - \left[(\gamma-1)g + \frac{dc^2}{dz}\right]\chi - \frac{1}{\rho_0}\frac{\partial s}{\partial z} \quad . \tag{A2}$$

When the time dependences of $u$, $w$, $p$, $\rho$, and $s$ are proportional to a common factor $e^{i\sigma t}$, a straightforward calculation leads to Equations 34, 35, and 36 from Equations A1, A2, and 33, respectively.

Differentiating Equations A1 and A2 with respect to $x$ and $z$, respectively, and adding them gives

$$\frac{\partial^2 \chi}{\partial t^2} = c^2 \nabla^2 \chi - g\frac{\partial \zeta}{\partial x} + \left(\frac{dc^2}{dz} - \gamma g\right)\frac{\partial \chi}{\partial z} - \left(\frac{dc^2}{dz} + \gamma g\right)\frac{1}{\rho_0 c^2}\frac{\partial s}{\partial x} - \frac{1}{\rho_0}\nabla^2 s \quad , \tag{A3}$$

where

$$\zeta = \frac{\partial w}{\partial x} - \frac{\partial u}{\partial z} \quad . \tag{A4}$$

Similarly, by differentiating Equations A1 and A2 with respect to $z$ and $x$, respectively, and subtracting the former from the latter,

$$\frac{\partial^2 \zeta}{\partial t^2} = -\left[\frac{dc^2}{dz} + (\gamma-1)g\right]\frac{\partial \chi}{\partial x} + \frac{1}{\rho_0 c^2}\left(\frac{dc^2}{dz} + \gamma g\right)\frac{\partial s}{\partial x} \quad . \tag{A5}$$

The elimination of $\zeta$ from Equations A3 and A5 results in

$$\frac{\partial^4 \chi}{\partial t^4} = c^2 \nabla^2 \frac{\partial^2 \chi}{\partial t^2} + g\left(\frac{dc^2}{dz} + (\gamma-1)g\right)\frac{\partial^2 \chi}{\partial x^2} - g\frac{\partial}{\partial x}\left[\frac{1}{\rho_0 c^2}\left(\frac{dc^2}{dz} + \gamma g\right)\frac{\partial s}{\partial x}\right]$$

$$+ \left(\frac{dc^2}{dz} - \gamma g\right)\frac{\partial}{\partial z}\left(\frac{\partial^2 \chi}{\partial t^2}\right) - \left(\frac{dc^2}{dz} + \gamma g\right)\frac{1}{\rho_0 c^2}\frac{\partial}{\partial z}\left(\frac{\partial^2 s}{\partial t^2}\right) - \frac{1}{\rho_0}\nabla^2\left(\frac{\partial^2 s}{\partial t^2}\right) \quad . \tag{A6}$$

Since it is assumed that $u$, $w$, $p$, $\rho$, and $s$ are proportional to $e^{i\sigma t}$, the elimination of the time derivative from Equation A6 gives Equation 37.

## Appendix B

## Solution of Equation 59 at z = 0

Applying the Fourier transform to Equations 34 and 35 gives

$$-\sigma^2 U = ikc^2 X - ikgW - \frac{ik}{\rho_0} S \quad , \tag{B1}$$

$$-\sigma^2 W = c^2 \frac{dX}{dz} - \gamma gX + ikgU - \frac{ik}{\rho_0} \frac{dS}{dz} \quad . \tag{B2}$$

where $U$ and $W$ are the Fourier transforms of $u$ and $w$. Solving these bilateral equations with respect to $U$ and $W$ yields

$$\left(\sigma^4 - k^2 g^2\right) U = -ikgc^2 \frac{dX}{dz} + ik\left(\gamma g^2 - \sigma^2 c^2\right) X + \frac{ik\sigma^2}{\rho_0(z)} S + \frac{ikg}{\rho_0(z)} \frac{dS}{dz} \quad , \tag{B3}$$

$$\left(\sigma^4 - k^2 g^2\right) W = -c^2 \sigma^2 \frac{dX}{dz} + g\left(\gamma\sigma^2 - k^2 c^2\right) X + \frac{k^2 g}{\rho_0(z)} S + \frac{\sigma^2}{\rho_0(z)} \frac{dS}{dz} \quad . \tag{B4}$$

Since $W(z = 0) = 0$ and $dS/dz\big|_{z=0} = S(z = 0) = 0$, from the above equations

$$\frac{dX}{dz}\bigg|_{z=0} = m(\sigma) X(0) \quad , \tag{B5}$$

where

$$m(\sigma) \; = \; g\left(\frac{\gamma}{c^2} - \frac{k^2}{\sigma^2}\right) \quad . \tag{B6}$$

Similarly, the Fourier transform of Equation 33 is

$$i\sigma P(k, z) = g\rho_0(z) W - c^2 \rho_0(z) X(k, z) + S(k, z) \quad , \tag{B7}$$

where

$$P(k, z) = \frac{1}{\sqrt{2\pi}} \int_{-\infty}^{\infty} e^{ikx} p(x, z)\, dx \quad .$$

## Solution for X(z = 0), Direct Calculation

From Equation 61

$$\frac{dX}{dz} = n_1 e^{n_1 z}\left[ C_1 - \frac{1}{2\mu}\int_0^z F(z')e^{-n_1 z'}dz'\right] + n_2 e^{n_2 z}\left[ C_2 + \frac{1}{2\mu}\int_0^z F(z')e^{-n_2 z'}dz'\right] . \tag{B8}$$

Using Equation B5, from Equation B8 we get

$$C_1 = -\frac{n_2 - m(\sigma)}{n_1 - m(\sigma)} C_2 . \tag{B9}$$

If we write

$$A_1 = C_1 - \frac{1}{2\pi}\int_0^z F(z')e^{-n_1 z'}dz'$$

and

$$A_2 = C_2 + \frac{1}{2\mu}\int_0^z F(z')e^{-n_2 z'}dz'$$

then from Equations B8 and B9, by assuming $h < 2H$,

$$A_1 e^{-\mu z} = \begin{cases} C_1 e^{-\mu z} \qquad \text{for } 0 \le z \le z_0 , \\[2em] \left[ C_1 + Q_0\dfrac{\sigma^4 - k^2 g^2}{2\mu c^2 \sigma^2}\dfrac{1}{n_1 + \beta}C^{-(n_1+\beta)z_0}\right]e^{-\mu z} + Q_0\dfrac{\dfrac{\beta}{h} + \dfrac{k^2 g}{\sigma^2 H} - k^2}{2\mu\ n_1 + \beta}C^{-\left[(1/h)-(1/2H)\right]z} \\[2em] \qquad\qquad\qquad\qquad\qquad\qquad\qquad\qquad \text{for } z_0 \le z < \infty , \end{cases} \tag{B10}$$

and

$$A_2 e^{+\mu z} = \begin{cases} C_2 e^{\mu z} \qquad \text{for } 0 \le z \le z_0 , \\[2em] \left[ C_2 - Q_0\dfrac{\sigma^4 - k^2 g^2}{2\mu c^2 \sigma^2}\dfrac{1}{n_2 + \beta}e^{-(n_2+\beta)z_0}\right]e^{\mu z} - Q_0\dfrac{\dfrac{\beta}{h} + \dfrac{k^2 g}{\sigma^2 H} - k^2}{2\mu\ n_2 + \beta}e^{-\left[(1/h)-(1/2H)\right]z} \\[2em] \qquad\qquad\qquad\qquad\qquad\qquad\qquad\qquad \text{for } z_0 \le z < \infty , \end{cases} \tag{B11}$$

where

$$Q_0 = \sqrt{\frac{2}{\pi}} \frac{\sin \lambda_0 k}{k} \frac{(\gamma - 1) q_0}{\rho_s hc^2} e^{z_0/h} \quad , \tag{B12}$$

and

$$\beta = \frac{1}{h} - \frac{1}{H} \quad . \tag{B13}$$

The term including $e^{\mu z}$ represents the waves whose amplitudes increase with height. The corresponding kinetic energies diverge to infinity provided that $N^2 > M^2$. On the other hand, if $N^2 < M^2$ this term represents inward-going waves.

Because of the boundary conditions listed in the section "Mathematical Treatment," the terms including $e^{\mu z}$ must vanish. Therefore

$$C_2 = Q_0 \frac{\sigma^4 - k^2 g^2}{2\mu c^2 \sigma^2} \frac{1}{n_2 + \beta} e^{-(n_2 + \beta) z_0} \quad . \tag{B14}$$

Putting this constant into Equation 61, for $z = 0$, gives

$$X(k, 0) = \sqrt{\frac{2}{\pi}} \frac{(\gamma - 1) q_0}{h c^4 c^2 \rho_0} e^{(z_0/2H) - \mu z_0} \frac{\sin \lambda_0 k}{k} \frac{\sigma^4 - k^2 g^2}{(n_1 - m)(n_2 + \beta)} \quad . \tag{B15}$$

The continuity of $W(k, z)$ and $P(k, z)$ at $z = z_0$ is satisfied by the above choice of constants, i.e., it can be shown that

$$\lim_{\epsilon \to 0} W\left(z_0 - \epsilon\right) = \lim_{\epsilon' \to 0} W\left(z_0 + \epsilon'\right) \quad ,$$

$$\lim_{\epsilon \to 0} P\left(z_0 - \epsilon\right) = \lim_{\epsilon' \to 0} P\left(z_0 + \epsilon'\right) \quad .$$

## Solution for X(k,0) by means of the Laplace Transform

By applying the Laplace transform with respect to $z$,

$$\tilde{X}(k, s) = \int_0^\infty e^{-sz} X(k, z) dz \quad , \tag{B16}$$

Equation 59 becomes

$$\left(s^2 - 2Ns + M^2\right) \tilde{X} - (s - 2N) X(0) - \left.\frac{dX}{dz}\right|_{z=0} = Q_0 \frac{e^{-(s+\beta) z_0}}{s + \beta} \left[s^2 - 2Ns - k^2 \left(1 - \frac{g}{\sigma^2 H}\right)\right].$$

By making use of the relation shown by Equation B5, this is

$$\tilde{X}(k, s) = \frac{(s - 2N - m)}{(s - n_1)(s - n_2)} X(0) + \frac{Q_0 e^{-(s+\beta)z_0}}{\beta + s} \left[ 1 - \frac{\sigma^4 - k^2 g^2}{(s - n_1)(s - n_2)c^2 \sigma^2} \right],$$   (B17)

where $n_1$ and $n_2$ are given by Equations 63 and 64; $m = m(\sigma)$ and $Q_0$ are given by Equations B6 and B12.

By making use of the inverse transform of Equation B16 the solution to Equation 59 is

$$X(k, z) = \left( \frac{2N - m - n_1}{2\mu} e^{n_1 z} - \frac{2N - m - n_2}{2\mu} e^{n_2 z} \right) X(0) + Q_0 e^{-\beta z} \theta(z - z_0)$$

$$- Q_0 \frac{\sigma^4 - k^2 g^2}{2\mu c^2 \sigma^2} e^{-\beta z_0} \left[ \frac{e^{n_2(z-z_0)}}{\beta + n_2} - \frac{e^{n_1(z-z_0)}}{\beta + n_1} + \frac{e^{-\beta(z-z_0)}}{(\beta + n_1)(\beta + n_2)} \right] \theta(z - z_0) .$$   (B18)

Because of the boundary conditions at $z = \infty$, the term proportional to $e^{\mu z}$ must vanish, i.e., from Equation B18

$$- \frac{2N - m - n_2}{2\mu} X(0) - Q_0 \frac{\sigma^4 - k^2 g^2}{c^2 \sigma^2} \frac{e^{-(\beta+n_2)z_0}}{2\mu(\beta + n_2)} = 0 .$$   (B19)

This gives the same solution as Equation B15. It should be noted that the above solution satisfies the conditions of continuity of $w(x, z)$ and $p(x, z)$ at $z = z_0$, although $u(x, z)$ and $s(x, z)$ are not continuous at $z = z_0$.

## Appendix C

# Evaluation of p(x, 0)

As can be seen from Equation B15 $X(k, 0)$ is an even function of $k$. Therefore, the substitution of Equation B15 into Equation 67 gives

$$\chi(x, 0) = \frac{2}{\pi} \frac{(\gamma - 1) q_0 \sigma^2}{h k_g^2 \rho_s c^4} e^{z_0/2H} \int_0^\infty e^{-\mu z_0} \frac{\cos xk \sin \lambda_0 k}{k} \frac{k_g^2 - k^2}{(n_1 - m)(n_2 + \beta)} \, dk \qquad (C1)$$

where

$$k_g = \frac{\sigma^2}{g} . \qquad (C2)$$

Since $\mu$ is a real function of $k$ for $k \geq k_c$ and complex for $0 \leq k < k_c$, where

$$k_c = \frac{\sigma}{c} \sqrt{\frac{\sigma^2 - \sigma_A^2}{\sigma^2 - \sigma_B^2}} \quad , \qquad (C3)$$

Equation C1 can be written

$$\chi(x, 0) = \chi_c(x, 0) + \chi_{nc}(x, 0) \quad , \qquad (C4)$$

where

$$\chi_c(x, 0) = \frac{2}{\pi} \frac{(\gamma - 1) q_0 \sigma^2}{h k_2^2 \rho_s c^4} e^{z_0/2H} \int_0^{k_c} e^{-i\eta z_0} \frac{\cos xk \sin \lambda_0 k}{k} \frac{k_g^2 - k^2}{(n_1 - m)(n_2 + \beta)} \, dk \quad , \qquad (C5)$$

and

$$\chi_{nc}(x, 0) = \frac{2}{\pi} \frac{(\gamma - 1) q_0 \sigma^2}{h k_2^2 \rho_s c^4} e^{z_0/2H} \int_{k_c}^\infty e^{-\mu z_0} \frac{\cos xk \sin \lambda_0 k}{k} \frac{k_g^2 - k^2}{(n_1 - m)(n_2 + \beta)} \, dk \quad . \qquad (C6)$$

The integrand of $\chi_{nc}(x, 0)$ has two singular points $\sigma/c$ and $\sigma^2/g$, corresponding to the two types of free oscillations of the noncellular mode which were pointed out by Pekeris* and have

*Pekeris, C. L., "The Propagation of a Pulse in the Atmosphere. II," *Phys. Rev.* 73:145-154, January 15, 1948.

39

been discussed earlier. Because of a steep exponential term $e^{-\mu z_0}$, however, contributions of these singularities to the integral is not as important as the contribution from the narrow band near $k \geq k_c$, where the exponential term is nearly unity.

The integrand of $x_c$ has no singularities but oscillates by the term $e^{-i\eta z_0}$. The main contribution arises from a narrow domain near $k \lesssim$ approx. $k_c$. Equation 68 can be written

$$p(x, 0) = p_c(x, 0) + p_{nc}(x, 0) \quad , \tag{C7}$$

where

$$p_c(x, 0) = p_r + i p_i \quad , \tag{C8}$$

$$\left| p_c(x, 0) \right| = \frac{2}{\pi} \frac{(\gamma - 1) q_0 \sigma}{h k_g^2 c^2} e^{z_0/2H} \left| \int_0^{k_c} e^{-i\eta z_0} \frac{\cos xk \sin \lambda_0 k}{k} \frac{k_g^2 - k^2}{(n_1 - m)(n_2 + \beta)} \, dk \right| = \sqrt{p_r^2 + p_i^2} \, , \tag{C9}$$

and

$$p_{nc}(x, 0) \approx \frac{2}{\pi} \frac{(\gamma - 1) q_0 \sigma}{h k_g^2 c^2} e^{z_0/2H} \int_{k_c}^{k_g} e^{-\mu z_0} \frac{\cos xk \sin \lambda_0 k}{k} \frac{k_g^2 - k^2}{(n_1 - m)(n_2 + \beta)} \, dk \quad . \tag{C10}$$